Energy 342 (2026) 139692

Contents lists available at ScienceDirect

Energy

journal homepage: www.elsevier.com/locate/energy

3E analysis of a combined photovoltaic plant and biomass-fueled trigeneration system for an apartment building operating under the Collective Self-Consumption scheme

Maurizio La Villetta [a,*], Daniele Piazzullo [b], Pietro Catrini [a], Antonio Piacentino [a], Michela Costa [b]

[a] Department of Engineering, University of Palermo, Viale delle Scienze, Palermo, 90128, Italy
[b] CNR-STEMS, Viale Marconi, 4, Naples, 80125, Italy

ARTICLE INFO

Keywords:
Renewable energy communities
Collective self-consumption
Biomass cogeneration
Photovoltaic
Dynamic simulation

ABSTRACT

Renewable Energy Communities represent a promising solution for addressing the energy demands of buildings, fostering local renewable generation and enabling the transition to sustainable urban systems. In this context, photovoltaic systems are generally considered the reference technology, with incentive mechanisms predominantly tailored to their deployment. However, the integration of multiple renewable energy sources could mitigate the inherent variability of solar energy, which is conventionally managed through large electrical storage. In this regard, this study proposes a 3E (energy, economic, and environmental) analysis for an apartment building served by a photovoltaic plant and a biomass-fueled trigeneration system operating under Collective Self-Consumption scheme. The proposed configuration includes an internal combustion engine fueled by woodchips (20 kW_e/40 kW_{th}), an absorption chiller (17.6 kW_c), a photovoltaic plant (20 kW_e) and an electrical storage (45 kWh_e). The performance of this system is investigated through Transient System Simulation software. A comparative analysis with a *reference scenario* made of a gas-fired boiler and air-to-air heat pump is carried out first, followed by a photovoltaic only system. The results show that an energy self-sufficiency index and a thermal self-sufficiency index equal to 89.1 % and 86.0 %, respectively, could be achieved. A −90.5 % reduction in carbon dioxide emissions is also found. A comparison with a photovoltaic-only system underlines that the joint use could lead to higher economic revenues (about 4 %) and lower payback time. The present work underlines the opportunities arising by the integration of multiple renewable energy sources in the framework of Renewable Energy Communities applications offering insights into the limits of current legislative framework.

1. Introduction

Renewable Energy Communities (RECs) offer a range of benefits, including improved energy efficiency through local energy production and consumption, reduced greenhouse gas emissions, and enhanced integration of Renewable Energy Sources (RES), all of which contribute meaningfully to environmental impact mitigation and the transition toward a more sustainable energy system [1]. The European Union (EU) has recently made substantial progress in establishing a supportive framework for the expansion of RECs, particularly through the 2019 "Clean Energy for All Europeans" package [2]. Declared objectives involve specific references to the energy transition, as well as promoting the role of individuals in participating in the electricity market by enabling both individuals and groups to generate, consume, share, and sell electricity. In this framework, the Renewable Energy Directive (RED) II 2018/2001 establishes general rules for Energy Communities (ECs). It obliges Member States to develop and implement national regulatory frameworks to support their development and operation [3]. The RED II clarifies the precise meaning of Renewable Energy Communities and Renewable Self-Consumers (RSC) within the Collective Self-Consumption (CSC) framework [4]. The REC_S and RSC in the CSCs are based on the concept of self-generation of renewable energy, but differ in the location of the systems. In the case of CSC, self-consumers are located within the same building or condominium. The energy produced can be shared by apartment buildings, and it is limited to the specific location where it is generated. In the case of REC_S, energy plants

* Corresponding author.
E-mail address: maurizio.lavilletta@unipa.it (M. La Villetta).

https://doi.org/10.1016/j.energy.2025.139692
Received 13 May 2025; Received in revised form 16 November 2025; Accepted 15 December 2025
Available online 17 December 2025

can be located close to each other, but not necessarily in the same building. Finland and Denmark have integrated the RED II into their legal frameworks, while Sweden, Norway, and Poland have yet to incorporate these concepts [5]. In Germany, the Renewable Energy Sources Act introduced stricter rules for citizen energy companies and renewable energy communities to prevent corporate capture and clarify ownership rights [6]. In the Netherlands, a new subsidy mechanism aimed at stabilizing energy prices for community projects was introduced [6]. In Spain, not all metered energy is billed at the retailer's prices, but part of it can be valorized at a different price. The sharing benefit is directly accounted for in each member's bill [7]. Finally, in Italy, the RED II was transposed into the Regulatory Framework by Article 42-bis of Law-Decree 162/2019 [8], and incentives were established by the Minister of Economic Development [9]. Recently, this legislative framework was further refined by the Minister of Environment and Energy Security (MASE) [10] and ARERA [11], by defining the new incentive mechanisms, criteria, and modalities for the granting of National Recovery and Resilience Plan (NRRP) contributions as well.

1.1. Scientific literature on ECs

Moving to the scientific literature, published papers primarily focus on RECs in residential and tertiary sectors utilizing PV plants, and only a limited number of works have provided quantitative analysis of the combined use of RESs. In this regard, as shown in Fig. 1, a high number of scientific papers published between 2018 and 2024 in the Web of Science and Scopus database report a combination of the words "renewable energy communities" and "photovoltaic system", in the title, abstract and keywords. Instead, as shown by the red bars in Fig. 1, a few papers have considered the combination of the words "renewable energy communities" and "photovoltaic systems" with other RES technologies, e.g. "biomass".

A literature review is here following performed to identify knowledge gaps in the framework of Energy Communities. Plaza et al. [12] compared two scenarios involving seven end-users located in the South of France, each with a 7 kW PV plant. They operate as independent self-consumers, sharing energy from all PV systems. The results indicate that while individual self-consumption allows prosumers to utilize 80 % of their solar energy and meet 16 % of their electricity needs, energy sharing enables the use of 99 % of the solar energy, covering 22 % of participants' overall energy requirements.Fleischhacker et al. [13] analyzed energy communities in Linz (Austria) that pool various energy resources, including renewables like solar and wind, to optimize the mix of energy sources and demand-side management. Fina et al. [14] developed a multi-objective optimization model to determine the optimal size of PV systems with storage across multiple apartments in Austria and Germany, to minimize annual electricity costs and maximize self-consumption. Ceglia et al. [15] studied a PV-based REC in Southern Italy, highlighting its capacity to lower the energy poverty index from 9.84 % to 5.25 % for a typical residential user. Dal Cin et al. [16] proposed optimized demand-side management of REC located in Padua (north-east of Italy) based on both economic and environmental criteria, achieving a CO_2 emissions reduction and an internal rate of return by nearly 45 % and exceeding 11 %, respectively. Giordano et al. [17] investigated energy sharing between two Italian university buildings equipped with 4 kW and 8 kW PV plants, and 6 kWh and 12 kWh storage systems, showing economic savings of 71 % due to a 28 % increase in energy self-consumption. Ceglia et al. [18] evaluated the benefits of Renewable Energy Communities in Southern Italy, involving a collective services center building and an industrial wastewater treatment plant. The work compares the community approach to a single end-user configuration and the current state where users rely entirely on the power grid. The authors modeled a PV plant, while users' electric energy demands were determined from electricity bills. The findings show that energy sharing increases self-consumption and self-sufficiency, reducing annual primary energy demand by 1.2 MWh/kW_p, avoiding CO_2 emissions by 84 tons and operational costs by 101 k€. Battaglia et al. [19] developed an application in residential and commercial buildings located in Naples (Italy) using PV, geothermal HPs, and electric vehicle charging stations. Three incentive schemes were examined according to the Italian policy framework. The study highlights that the remuneration from recharging stations outperforms the incentives provided by RECs. Cirone et al. [20] examined a real case study of a REC located in a mountain region of Southern Italy. The heating system consists of electric air-water HPs assisted by a PV generator and an electric storage system. The work indicates that the RECs can reduce annual energy costs and CO_2 emissions when an optimal size of the plant technology is identified, and the renewable energies are transferred and shared among participants.

Other authors extended the analysis by including thermal energy in Energy Communities. For instance, Fouladvand et al. [21] and Papatsounis et al. [22] focused on thermal ECs. Ceglia et al. [23] analyzed a REC in Tirano municipality (Northern Italy) with an organic Rankine cycle biomass-based cogeneration plant, a mini-hydro plant, and a distributed photovoltaic system. An economic analysis was performed by considering the sale tariff for the shared electricity within the community and a variable tariff for the thermal energy delivered to the district heating network. By considering that the thermal energy can be sold and the cogenerator works at full power load, the results show that the economic feasibility of wood-biomass-based renewable energy communities under the current Italian regulatory framework can contribute to the development of initiatives aimed at promoting all renewable technologies, also with a higher rate of national component than photovoltaic, to enhance the local resources of each territory. Kim et al. [24] conducted a techno-economic analysis of a hybrid renewable system for a net-zero energy community located in Jincheon (South

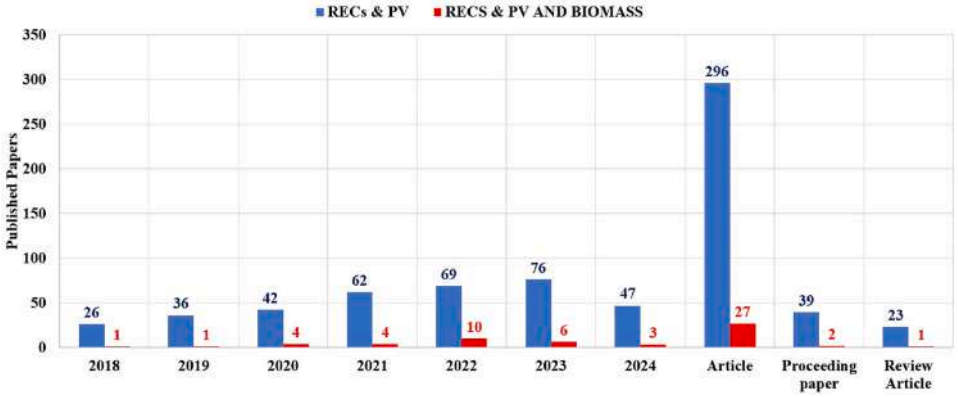

Fig. 1. Number of scientific papers in Web of Science and Scopus Database from 2018 to 2024 on RECs with PV and Biomass plants.

Korea), incorporating solar thermal systems, seasonal thermal energy systems, heat pump systems (HPs), and district heating networks. Results showed that increasing the solar fraction in the proposed system significantly reduces CO_2 emissions and increases primary energy savings, with a payback period of six years. Ancona et al. [25] explored the potential of RECs integrated with district heating networks in Corticella (Italy), enhancing internal energy sharing through PV systems and HPs to boost self-consumption and investment efficiency. Their findings indicate significant reductions in energy demand, emissions, and costs. Similar conclusions were achieved by Ceglia et al. [26] for a case study in Naples (Southern Italy), regarding a small REC of two offices. Ceglia et al. [27] investigated different scenarios of a biomass-based cogeneration system, a small hydropower plant, and a distributed photovoltaic system for REC application in Northern Italy. The results show that the annual renewable electricity used to satisfy electric load increases by 20.3 % and about 68.1 % of the total thermo-electric requests were met through biomass utilization. The bi-directional interactions with the power grid were reduced from 60.6 % to 51.7 %. The thermal and electric sharing within the community ensures a decrease in carbon dioxide emissions by up to 18.5 %.

1.2. Research gap, novelty, and contribution of the present study

The previous review reveals that only a limited number of studies have addressed the joint use of different RES technologies within the framework of ECs [19,23,27]. In this respect, PV is typically assumed as reference technology, and even when a combination of RES technologies is adopted, the focus is often on very large-scale systems [23]. In addition, the potential benefits of small-scale CHP plants in Renewable Energy Communities are negligible. Worth noting that combining different RES technologies can enhance energy production, sharing, and self-consumption, while also mitigating the daily and seasonal variability of some RESs [23,28]. In this context, biomass-fueled technologies can complement PV or wind systems by providing electricity during periods of low solar or wind availability, such as at night, while valorizing an energy source that is often underutilized [29]. Furthermore, when operated in polygeneration mode, these technologies can supply heating and cooling to end users, leading to greater energy savings, reduced emissions, and increased economic revenues for plant owners due to avoided fuel costs [30,31]. In the case of ECs, there is a gap in understanding the potential contributions of RES technologies beyond PV, both in terms of enhancing energy and economic performance (e.g., increased self-sufficiency, improved electricity sharing, and higher revenues), and in terms of identifying potential barriers, such as the need for thermal energy storage or the development of tailored financial support mechanisms. In this respect, this study proposes a 3E (energy, economic and environmental) analysis assumed as a condominium with a Photovoltaic (20 kW_p), and biomass micro Combined Heat and Power (mCHP) (20 kW_e/40 kW_{th}) fueled with woodchip system and equipped with a Water-Fired Absorption Chiller (WFAC) (17.6 kW_c) and electrical storage (45 kWh_e), operating under a Collective Self-Consumption scheme. Through a yearly analysis performed within the TRaNsient SYstems Simulation (TRNSYS) [32], energy and economic analyses were realised considering the incentive tariff currently available for ECs in Italy. Results are also compared to those achieved by a gas-fired boiler and split units and a PV-only system, which are commonly used in residential buildings. The following contributions could be identified.

i. For the first time, the energy and economic benefits of small-scale biomass-fueled polygeneration systems operating under RECs are investigated. In this context, the ability to share electricity among users may support the wider adoption of these systems, which typically require continuous operation at full load. At the same time, potential drawbacks, such as the limited ability to utilize recovered thermal energy, are examined to highlight existing weaknesses and identify areas for future research (e.g., the necessity to include thermal energy storage, or developing thermal energy sharing strategy).
ii. An analysis of the effects of the current incentive tariff is proposed to assess its impact on the feasibility of investments in energy systems other than PV systems, for which the legislative framework on RECs and CSCs is typically designed. Through comparative analysis with reference systems (made up of boilers and split units), insights into the strengths and limitations of the existing legislative framework are provided, aiming to highlight key issues and propose potential refinements for future policy development.
iii. A comparison of energy and economic results with ECs based on only PVs is performed to better comprehend the benefits and drawbacks of the combined use of RES in the framework of RECs.

The remainder of this paper is structured as follows. The second section provides details of the reference Collective Self-Consumption, with a description of the modeling of each subsystem. In the third section, simulated scenarios are presented, along with indicators. In the fourth section, results are shown and discussed. Finally, conclusions are briefly drawn.

2. Material and methods

As previously mentioned, the supporting mechanism introduced for RECs by the MASE is assumed as reference [33]. For the sake of completeness, some details are here provided, to clarify the energy and monetary flows that will be discussed in the following [33].

First, it is important to clarify the definition of energy self-consumption and energy sharing in the Italian regulations for Renewable Energy Communities and Renewable Self-Consumers within the Collective Self-Consumption [34]. In this respect, a scheme is reported in Fig. 2 for the case of a Collective Self-Consumption consisting of an apartment building with a RES plant. However, this consideration can be easily extended to the case of Renewable Energy Communities. The following energy flow could be identified.

- *physical energy self-consumption* "Ec_ϵ"– is the energy produced by the RES plant that is directly consumed by the Collective Self-Consumptions [34] through a "physical connection" (i.e., via electrical cables) to the same Point Of Delivery (POD) as the RES plant. Typically, this is less or equal to the amount of energy required to operate the common zones of the buildings, indicated as E_c in Fig. 2,

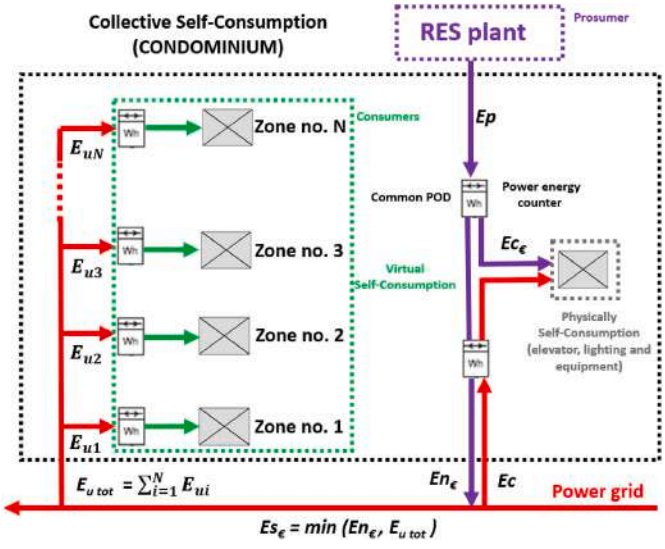

Fig. 2. Collective Self-Consumption scheme: representation of energy flows.

such as the elevator, lighting, and equipment from corridor zones of the building, and electric vehicle charging stations. As shown in Eq. (1), $Ec_€$ is equal to the energy produced by the RES plant (E_p), if E_p is lower than E_c. Conversely, $Ec_€$ is equal to E_c.

- *energy sharing as virtual self-consumption* "$Es_€$" – is the amount of energy from the RES plant that a Renewable Energy Communities or Collective Self-Consumptions, virtually shares with other members of the community after meeting its own electricity needs. According to Ref. [8], the energy shared in a given period $Es_€$ (see Eq. (2)) is the "minimum" value between the net electrical energy produced and fed into the grid by the RES plants ($En_€$) and the electrical energy withdrawn from the thermal zones of the reference building $E_{u\ tot}$ (i.e., the energy required by apartments for lighting and other devices, air conditioning, and so on). As shown in Eq. (3), $En_€$ is the difference between the total electrical energy produced by RES (E_P) and the physical self-consumption energy consumed ($Ec_€$).

$$Ec_€ = \begin{cases} Ec, if\ E_p \geq Ec \\ E_p, if\ E_p < Ec \end{cases} \quad (1)$$

$$Es_€ = min\ (En_€, E_{u\ tot}) = min\left(En_€, \sum_{i=1}^{N} E_{ui}\right) \quad (2)$$

$$En_€ = \begin{cases} (E_p - Ec_€), if\ (E_p - Ec_€) > 0 \\ 0, if\ (E_p - Ec_€) \leq 0 \end{cases} \quad (3)$$

According to Ref. [10], the shared energy $Es_€$ is sold at incentive tariff T_p, which remains fixed for 20 years. As shown in Eq. (4), T_p consists of: (i) a fixed component, $T_{p,fix}$, equal to 60, 70, or 80 €/MWh depending on whether the RES plant's electrical capacity is lower or equal to 200 kW_e, 600 kW_e, and 1 MW_e, respectively; and a (ii) a variable component, (indicated as "max (0; 180 − P_z)" in Eq. (4)) that decreases as the zonal energy price (P_z) increases, reaching zero when P_z equals or exceeds 180 €/MWh. However, T_p cannot exceed a maximum value of €100, €110, or 120 €/MWh, also based on the plant's nominal electrical capacity (is lower or equal to 200 kW_e, 600 kW_e, and 1 MW_e, respectively)

$$T_p = T_{p,fix} + \max\ (0;\ 180 - P_z) \quad (4)$$

In addition, two further contributions are introduced.

- An incentive of 4 €/MWh is granted to plants located in the central part of Italy to compensate for the lower insolation (Lazio, Marche, Toscana, Umbria e Abruzzo). Conversely, the incentive is 10 €/MWh in Northern Italy (Emilia-Romagna, Friuli-Venezia Giulia, Liguria, Lombardia, Piemonte, Trentino-Alto Adige, Valle d'Aosta, Veneto).
- A tariff related to the appreciation of self-consumed energy indicated as T_{ARERA}, is introduced to account for avoided loss in the national power grid. Details on the calculation of T_{ARERA} are here omitted and limited to Appendix A. However, as will be shown, it does not heavily affect the economic results, since it accounts for less than 10 %.

The renewable electricity produced and fed into the grid, $En_€$ can be sold to the *Gestore dei Servizi Energetici* (GSE) using dedicated withdrawal, with a selling price set equal to the zonal price, P_z (€/MWh).

2.1. Description and modelling of the reference collective self-consumption scheme

The paper proposes a Collective Self-Consumption based on an apartment building, a biomass-fueled micro Combined Heat, Cooling and Power (PV-Biomass mCHCP) system consisting of a PV plant, a Lithium battery and an internal combustion engine (ICE) integrated with a Water-Fired Absorption Chiller. A simplified scheme is shown in Fig. 3. Specifically, the ICE provides thermal energy that is directly used for biomass drying and space heating in winter or to drive the WFAC in summer to produce cold water for space cooling. The electricity from ICE is mainly shared by the apartments. Conversely, the electricity from the PV plant is shared, sold to the grid, or stored in the battery. The green box in Fig. 3, indicated as "*Base Case*", includes natural-gas boilers and split units, that are used to meet the heating and cooling demand of the apartments before the inclusion of the RES plant.

A model was developed in the TRNSYS v. 17.0, to quantify (i) the heating and cooling demands of the buildings, and (ii) the operation of the energy plant. In the following, a description of each component along with its modelling is provided.

2.1.1. Description and modelling of the reference building

The reference building is characterized by 4 floors, 32 apartments, 1 office, and 4 corridors (see Table 1) located in Palermo, Southern Italy.

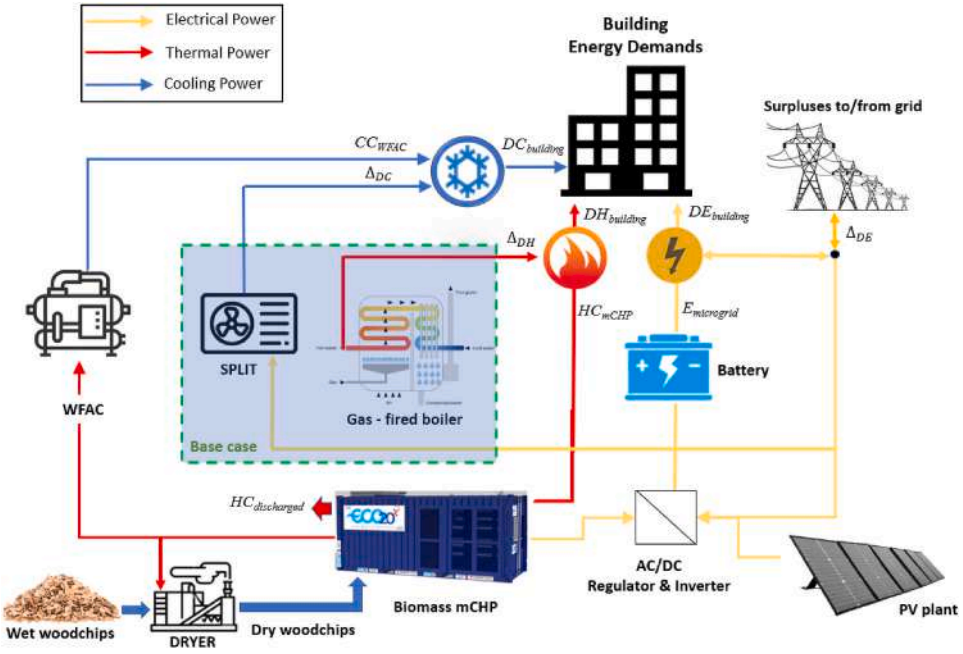

Fig. 3. Scheme of the reference Collective Self-Consumption scheme.

Table 1
Properties of the reference building according to ASHRAE 90.1 and UNI/TR 11552:2014.

Geometrical properties and internal gains of the building according to ASHRAE 90.1 [36]	
Net conditioned floor [m^2]	2824
Number of floors	4
Window-Wall-Ratio (WWR) [%]	20
Number of thermal zones	33
Lighting [W/m^2]	14
Electric equipment [W/m^2]	11
Occupants [m^2/person]	33
Thermal properties of envelope according to UNI/TR 11552:2014 [37]	
Ground [W/m^2K] – Code entity	1.26 – SOL08
External wall [W/m^2K] – Code entity	0.6 – MCV04
External roof [W/m^2K] – Code entity	1.62 – COP04
Adjacent wall [W/m^2K] – Code entity	1.18 – MLP03
Adjacent ceiling [W/m^2K] – Code entity	1.68 – SOL02
Windows [W/m^2K] – Code entity	1.06 – TRNSYS library

The geometry and orientations of walls and windows were defined in SKETCHUP [35] and then imported in TRNSYS into Type 56 (multi-zone building). The schedules of internal gains, such as people, lighting, and electrical devices, were defined following ASHRAE 90.1–2016 [36]. Conversely, the thermal properties of the envelope were adapted to the Italian building stock by using the Italian Standard UNI/TR 11552:2014 [37]. Table 1 summarizes the most important properties.

Fig. 4a shows the yearly thermal ($DH_{building}$) and cooling ($DC_{building}$) demands of the building obtained from TRNSYS. A 67.5 kW_{th} peak in the heating demand was observed. A 52.4 kW_c peak in the cooling demand was found. Fig. 4b shows the weekly electricity demand ($DE_{building}$) for lighting and other equipment in winter, obtained from the simulation. This trend is almost the same during the year according to the daily schedules by ASHRAE 90.1–2016.

2.1.2. Description and modelling of the prime mover

Before describing the reference prime mover of the PV-Biomass mCHCP plant, it is essential to outline the procedure used to determine its nominal capacity. The profitability of the proposed systems is strongly influenced by plant design, operational strategies, and external factors such as energy prices and the availability of support mechanisms [38]. However, the economic feasibility must be carefully assessed considering the inherent limitations of each plant component. Indeed, biomass-fueled ICEs operate differently from those powered by natural gas. In the latter, the use of high-purity natural gas enables precise control strategies, allowing the prime mover to modulate its output in response to the user's thermal demand (commonly referred to as "heat tracking mode"), reducing the waste of thermal energy. It follows that a sizing approach based on the combined use of Aggregate Thermal Demand (ATD) of the users and its Full Load Energy Curve (FLEC), ensures

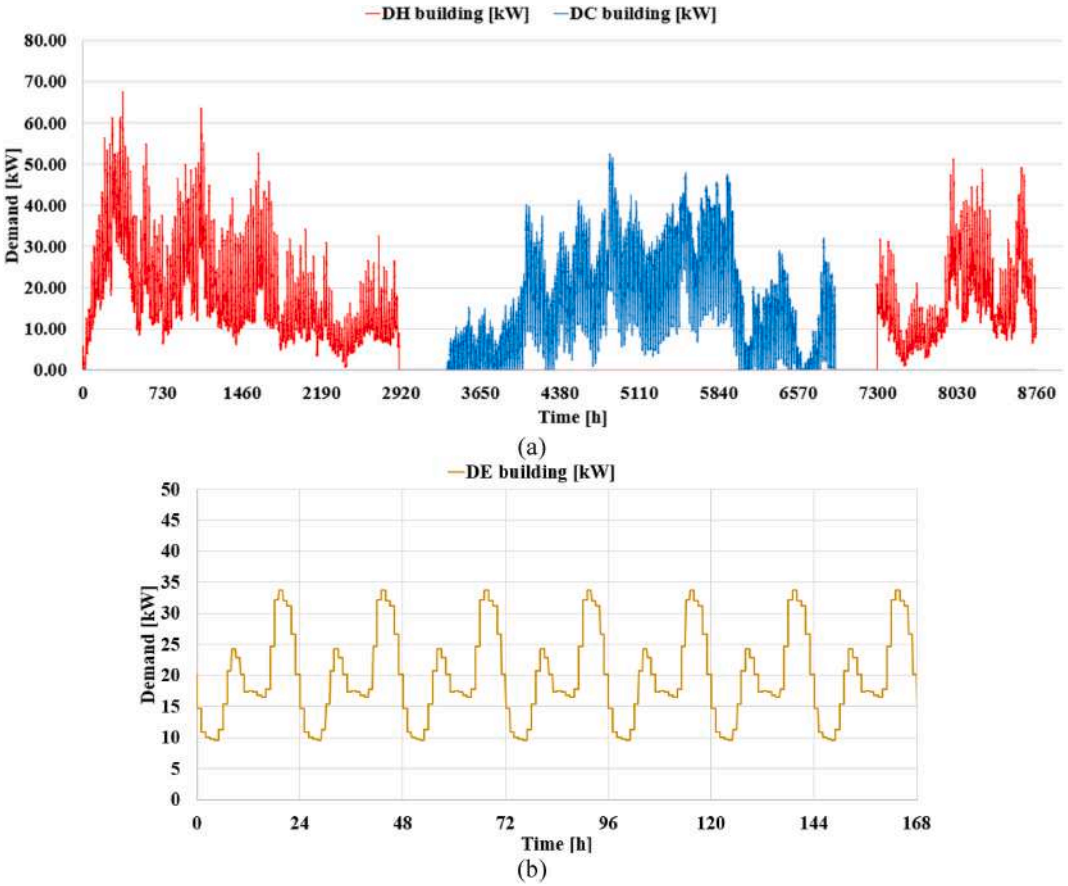

Fig. 4. Energy demands of the reference building: (a) yearly thermal and cooling demands, (b) weekly electricity demand in winter.

energy savings and economic profitability [38,39].

In the case of biomass ICEs operating with low-purity syngas, the strong dependence of the prime mover performance on the quality of the supplied syngas makes refined control hard to implement. Specifically, the performance of the prime mover is influenced by biomass quality (e.g., type, blending, particle size, etc.) and other process parameters (such as gasification temperature, equivalence ratio, tar formation, pressure drops, etc.) [40]. For these reasons, manufacturers of biomass CHP plants, especially in the case of small-scale applications (<50 kW_e), tend to control these systems by maximizing the electricity produced instead of tracking the thermal demand of the user [41]. Such a choice ultimately results: (i) in a loss of thermal energy recovered from the mCHP during periods of low thermal demand, a situation that can be justified using biomass, which, if not employed for this purpose, might be otherwise burned and wasted; and (ii) a surplus in electricity production which can be sold to the grid, or which could become even profitable in the case of energy sharing as in RECs.

Based on the previous consideration, in the present work, the nominal capacity of the biomass prime mover was selected on the cumulative curve and FLEC for the electricity demand of the user rather than the ATD. More specifically, using the demands of the reference building resulting from Type 56, in Fig. 5a the cumulative curve for electricity demand (dashed gold line) is presented. In addition, cumulative curves for the heating (solid red line), cooling (solid light blue line) demands, and ATD curve (dashed blue line) are shown. The ATD was obtained by summing the thermal demands for space heating and biomass drying, and the demand of a WFAC used to meet the space cooling demand, featured by an average COP_{WFAC} equal to 0.7.

Fig. 5b plots the FLEC for the electric demand, the ATD, and the cooling demand.

The size of the prime mover is capacity Y_P that maximizes the hours of operation X_P along the cumulative energy curve (Fig. 5a), and the area ($X_P \bullet Y_P$) corresponds to the total annual energy output (heat, cooling, or electricity) running the prime mover at full load [38,39]. In the case of electricity, FLEC in Fig. 5b (yellow curve) has a 16.51 kW_e peak. Conversely, in the case of a FLEC derived from the ATD, the size Y_P that maximizes thermal energy recovery at full load is equal to 18.48 kW_{th}. Then, assuming an ICE with an average Power-to-Heat Ratio (PHR_{ICE}) of 0.5 (i.e., half of the engine's thermal power), the resulting electrical output would be equal to about 9 kW_e. Although this size would lead to low thermal energy waste, it would result in very low electrical energy production, maybe reducing the benefits arising from Collective Self-Consumption, where self-consumed and shared electricity is necessary. Such a choice ultimately results in a loss of thermal energy recovered from the mCHP during periods of low thermal demand, which will be quantified and justified in the following using ad-hoc indicators.

It is unlikely that the optimal size (i.e. 16.51 kW_e) could be found in commercial catalogs. Therefore, it is preferable to define not a specific size, but rather an optimal range, ensuring that the energy supplied at full load remains below 80 % of the maximum capacity. For example, if the peak power is 16.51 kW_e, the corresponding maximum annual energy production is 102512.67 kWh. 80 % of this value is 82010.13 kWh, which corresponds to a power close to 20 kW_e. Following the FLEC analysis, a literature review was conducted on biomass mCHP systems commercially available in Italy. The review revealed that the CMD ECO20x offers technical characteristics suitable for the intended purpose. It is characterized by electric and thermal power equal to 20 kW_e and 40 kW_{th}, respectively [42].

The mCHP system was modeled using both the manufacturer's data (Table 2) and a performance map implemented in Type 907. The map was developed using the results of a previously zero-one dimensional (0-1D) model of the engine, which solves the Navier Stokes equations, employing a complex approach in the combustion chamber for the prediction of engine performance [43]. The engine intake air temperature was assumed to be equal to the outdoor temperature included in the Metereonorm Weather data file (Type 15-2). Validation was previously performed in Refs. [44,45] by some of the authors of this paper.

Biomass must undergo thermal pre-treatments to ensure its suitability for gasification technologies [47]. Therefore, part of the thermal energy recovered from the mCHP plant can be used for the drying process to improve fuel quality by reducing its moisture content. The thermal energy required for drying was evaluated through an energy

Table 2
Nominal parameters of the mCHP and schedules.

Sub-section	Nominal parameters	Plant management schedule	
		Yearly	Daily/Weekly
mCHP [42, 46]	Power-to-Heat Ratio PHR_{ICE} = 0.5 Electric power = 20 kW_e Thermal power = 40 kW_{th} Mass flow rate to user = 1 kg/s (heating season) Mass flow rate to the generator of the absorption chiller = 1 kg/s (cooling season)	Heating season: Nov 1 – May 1 (ON) Cooling season: May 15 – Oct 15 (ON) Intermediate May 2 - May 14 (OFF) Oct 16 - Oct 31 (OFF)	Full-load operations in the heating and cooling season: - for 6 days (Mon – Sat); - on Sunday, the mCHP stops for 8 h (08:00–16:00) for maintenance

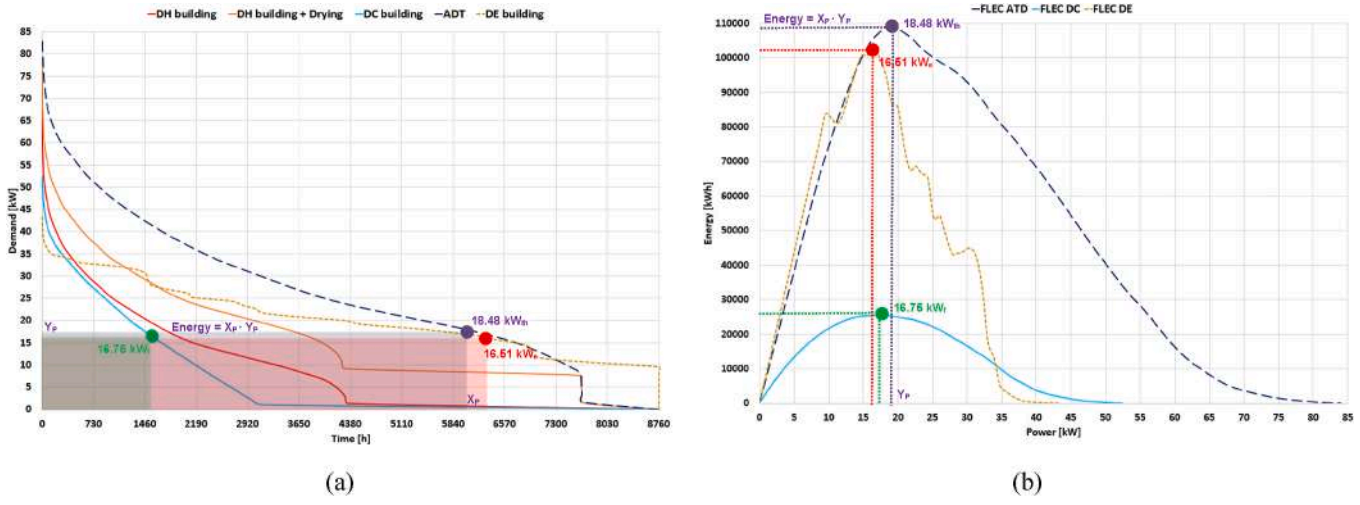

Fig. 5. (a) Cumulative energy demand curves, and (b) full-load energy curves.

balance, assuming a reduction in moisture content from 50 % to 20 %. In Fig. 6 some details of the process are provided.

2.1.3. Description and modelling of the absorption chiller

The nominal cooling capacity of the WFAC was selected using the peak value of FLEC for the cooling demand shown in Fig. 5b. A nominal capacity equal to 16.75 kW_c was required. Then, the Yazaki Water-Fired single-effect chiller (model: WFC-SC5) [48] with a rated cooling capacity of 17.6 kW_c was selected. Table 3 shows details of the reference WFAC available from the manufacturer.

The performance of the WFAC was modeled using data based on the manufacturers. The cooling capacity (P_{EVAP}) and the COP_{WFAC} were calculated by available maps, here shown in Fig. 7a-c. Maps were developed in terms of a Cooling Capacity Factor (CCF), a Heat Input Factor (HFI), and a Flow Correction Factor (FCF), with the following boundary conditions: (i) temperature of the generator ranging from 70 °C to 95 °C; (ii) cooling water temperature supplied to the condenser equal to 27 °C, 29.5 °C, and 31 °C; and (iii) chilled water outlet temperature of 7 °C. The FCF also depends on the percentage variation of heat medium flow to the nominal value.

These maps were implemented in the TRNSYS through Multi-Dimensional Data Interpolation (Type 581c), and the absorption chiller heat balance was performed according to the following equations proposed by manufacturers [48]:

$$P_{EVAP} = CCF \cdot FCF \cdot RCC \quad (5)$$

$$P_{GEN} = HIF \cdot FCF \cdot RHI \quad (6)$$

$$P_{CND} = P_{EVAP} + P_{GEN} \quad (7)$$

$$COP_{WFAC} = \frac{P_{EVAP}}{P_{GEN}} \quad (8)$$

where: RCC is the Rated Cooling Capacity of evaporator and RHI is the Rated Heat Input of generator (see Table 3).

2.1.4. Description and modelling of the photovoltaic plant and lithium battery

The nominal capacity of the PV plant was assumed to be 20 kW_p according to the annual electric demand from the building and the possible support offered to the electricity production during the maintenance of the biomass-fueled mCHP system (e.g. within the 08:00 to 16:00 time slot every Sunday).

The PV plant was modeled in TRNSYS by using Type 194, where the five-parameters equivalent circuit (the light current I_L, the diode reverse saturation current I_0, the series resistance R_s, the shunt resistance R_{sh} and the ideality factor α function of the cell temperature) is solved to evaluate the current-voltage relationship of a single solar cell or a complete array [49,50]. In the reference PV system, the parameters were determined by values provided by the manufacturer at standard reference conditions [51]. An inverter and a regulator were considered in the model to properly manage the AC/DC power coming from the ICE and the PV systems. Type 47 specifies how the battery's State Of Charge (SoC) varies over time, given the rate of charge or discharge [46]. The efficiencies of the inverter and the regulator were imposed as equal to 95 % and 96 %, respectively. A maximum and minimum SoC was imposed equal to 95 % and 5 % for the storage system. Indeed, the battery SoC should be higher than 5 % for safety issues, while all the excess power produced and supplied to the battery at an SoC higher than 95 % is directly fed to the national grid. Lastly, it was assumed that the efficiency of battery charging and discharging was equal to 98 %.

Table 4 collects information from manufacturers used in the TRNSYS model.

Table 3
Nominal parameters of the WFAC and schedules.

Sub-section	Nominal parameters	Plant management schedule	
		Yearly	Daily/Weekly
Absorption chiller [48]	- Coefficient of Performance COP_{WFAC} = 0.70 - Rated Heat Input (generator) = 25.1 kW_{th} - Hot water temperature IN/OUT = 88 °C/83 °C obtained from mCHP system - Hot water flow rate = 1.2 kg/s - Rated Cooling Capacity (evaporator) = 17.6 kW_f - Chilled water temperature IN/OUT = 12.5 °C/7 °C - Chilled water flow rate = 0.77 kg/s - Heat rejection (condenser) = 42.7 kW_{th} - Cooling water temperature IN/OUT = 31 °C/35 °C (obtained from cooling tower) - Cooling water flow rate = 2.55 kg/s	Only cooling season: May 15 – Oct 15 (ON)	Full-load only during the cooling season and when the mCHP unit is in operation.

2.1.5. Modeling of the "base case"

As previously mentioned, to better examine the potential benefits of the proposed plant, a conventional "Base case" system was assumed, consisting of: (i) gas-fired boilers and split units to meet the heating and cooling demand; and (ii) the power grid to cover to electrical demand (see Fig. 3). The fuel consumption of the gas-fired boiler was calculated using both the instantaneous heating demand values from the building model developed in TRNSYS and the boiler efficiency η_{boil} equal to 82.0 % [53]. Similarly, to estimate the electricity consumption during

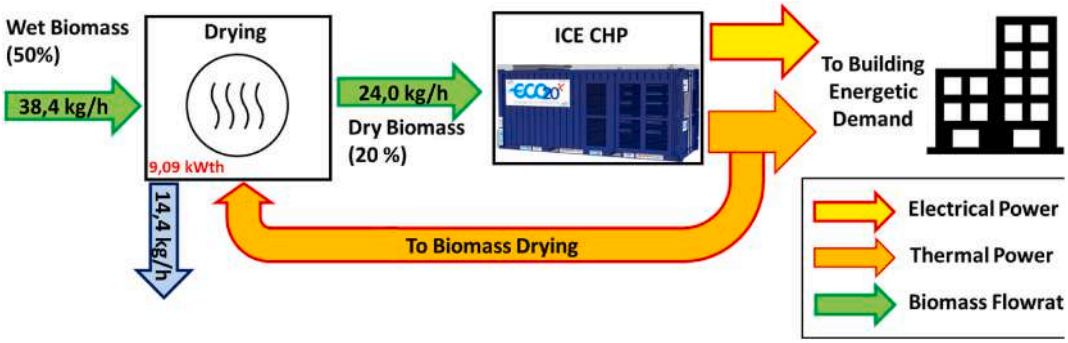

Fig. 6. Energy balance related to the biomass drying pre-treatment.

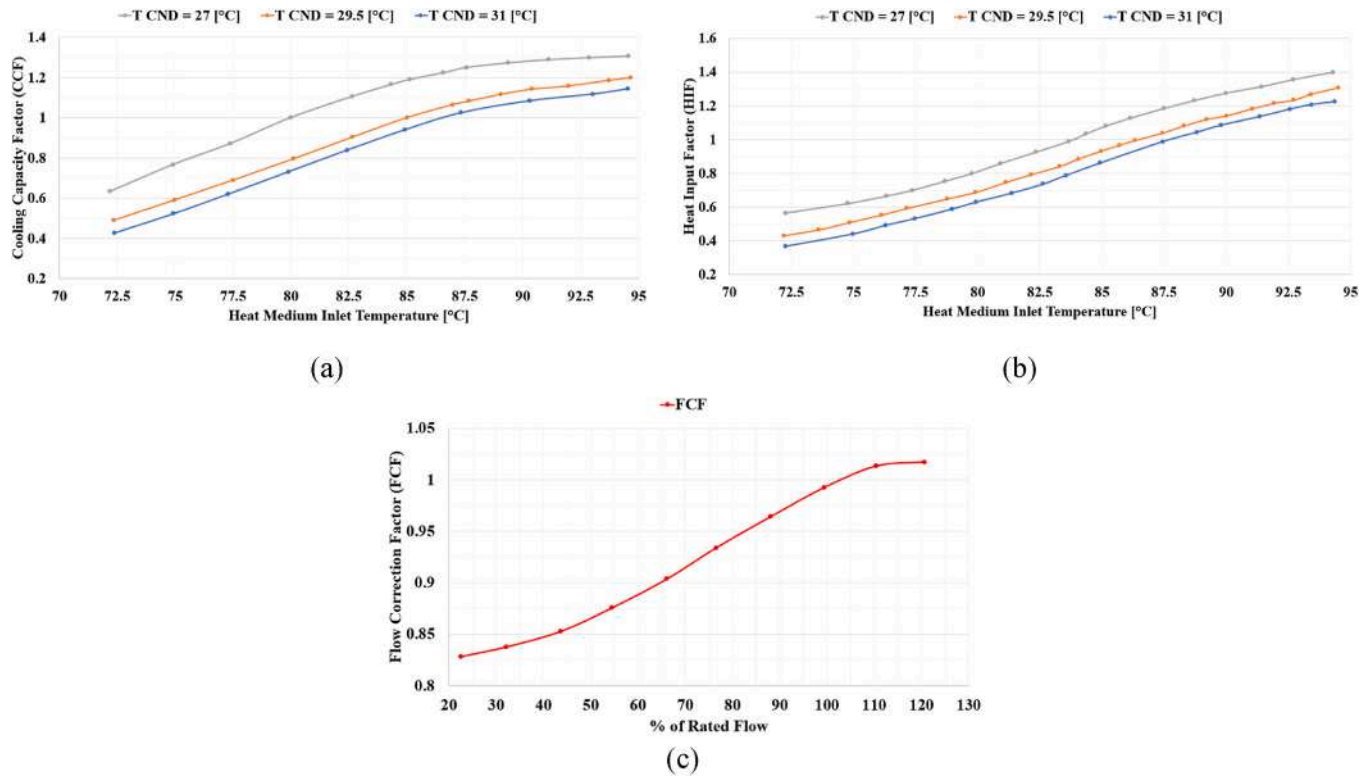

Fig. 7. Performance of Yazaki Water-Fired single-effect chiller, model: WFC-SC5: a) cooling capacity factor (CCF), b) heating input factor (HIF), c) flow correction factor (FCF). The performances are evaluated at the rated chilled water outlet temperature of 7 °C [48].

Table 4
Nominal parameters of the PV plant and Lithium battery, and schedules.

Sub-section	Nominal parameters	Plant management schedule
PV systems [51]	- Data PV module = 405 W–2 m^2, - Architecture = 10 PV modules arranged in series and 5 strings arranged in parallel - Power of PV system = 20.25 kW_e	Full-load operations over the years
Battery [52]	- Data cell (lithium battery) = 16.7 Ah, 2.8 V - Capacity = 45.17 kWh	Full-load operations over the years

summer for the split systems, both the instantaneous cooling demand from TRNSYS and the Energy Efficiency Ratio (EER) by CLIVET Cristallo unit (model: S.IM1+MM1-Y 35M) were used. Manufacturer data, provided as a performance map based on condenser temperatures (25–45 °C) and evaporator temperatures (23.5–30.5 °C), were retrieved (see Fig. 8) [54]. This map was implemented in TRNSYS using Type 581c.

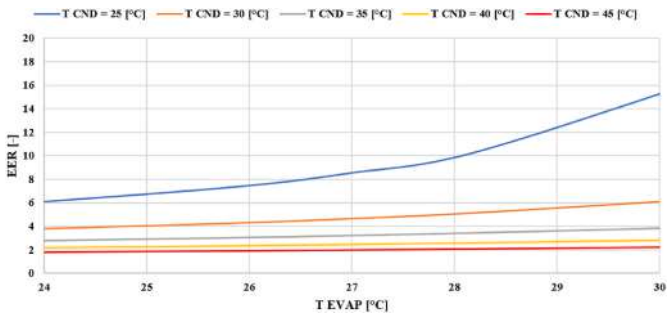

Fig. 8. Performance of Clivet Cristallo, model: S.IM1+MM1-Y 35M [54].

3. Description of simulated scenarios and indicators

Fig. 9 summarizes the flowchart of the microgrid developed in TRNSYS. During the dynamic simulation and for each timestep *t*, the $DH_{building}$, $DC_{building}$ and $DE_{building}$ from Type 56 were imported into the microgrid model using Type 9e. Simulations were performed assuming a 1-h timestep.

Regarding the operation strategy of the microgrid adopted, Fig. 10 provides a description for the heating and cooling season and for electricity.

Four scenarios were simulated to examine the effects of the incentive on the profitability of the investment. As shown in Table 5 and Fig. 11, the scenarios allow understanding (i) the sensitivity of the profitability of the investment to variation of the incentive tariff in the case of variation of the zonal price (effects demand and RES penetration in the generation mix), (ii) the capability of the mechanism to support deployment of RECs based on RES technologies other than PV. More specifically, a *best-case scenario*, here indicated as S_1, is characterized by a high zonal price P_z, i.e., 180 €/MWh, which leads (according to Eq. (1)) to the lowest T_p value (i.e., 80 €/MWh). This scenario can be assumed as the *reference* one for the establishment of RECs and the deployment of RES systems. On the other hand, the S_5 scenario represents the *worst case*, because it leads to lower incomes from the energy sold to the grid with respect to S_1, as testified by the lowest zonal price, 60 €/MWh, typically observed before crisis. As shown in Table 5, three *intermediated scenarios* (S_2, S_3,and S_4) were also included, to evaluate the sensitivity of economic results to the electricity zonal price.

Considering the total electric capacity of the assumed RES plant (40 kW_e), the incentive tariff T_p = 80 + max (0; 180 - P_z). The addition incentive based on insolation is null (Palermo is in the Sud of Italy) and the T_{ARERA} was set equal to 9.08 €/MWh. Worth noting that in each scenario, the incentive tariffs and the revenues from dedicated withdrawal from GSE were computed, accounting for the defined discount and fuel inflation rate.

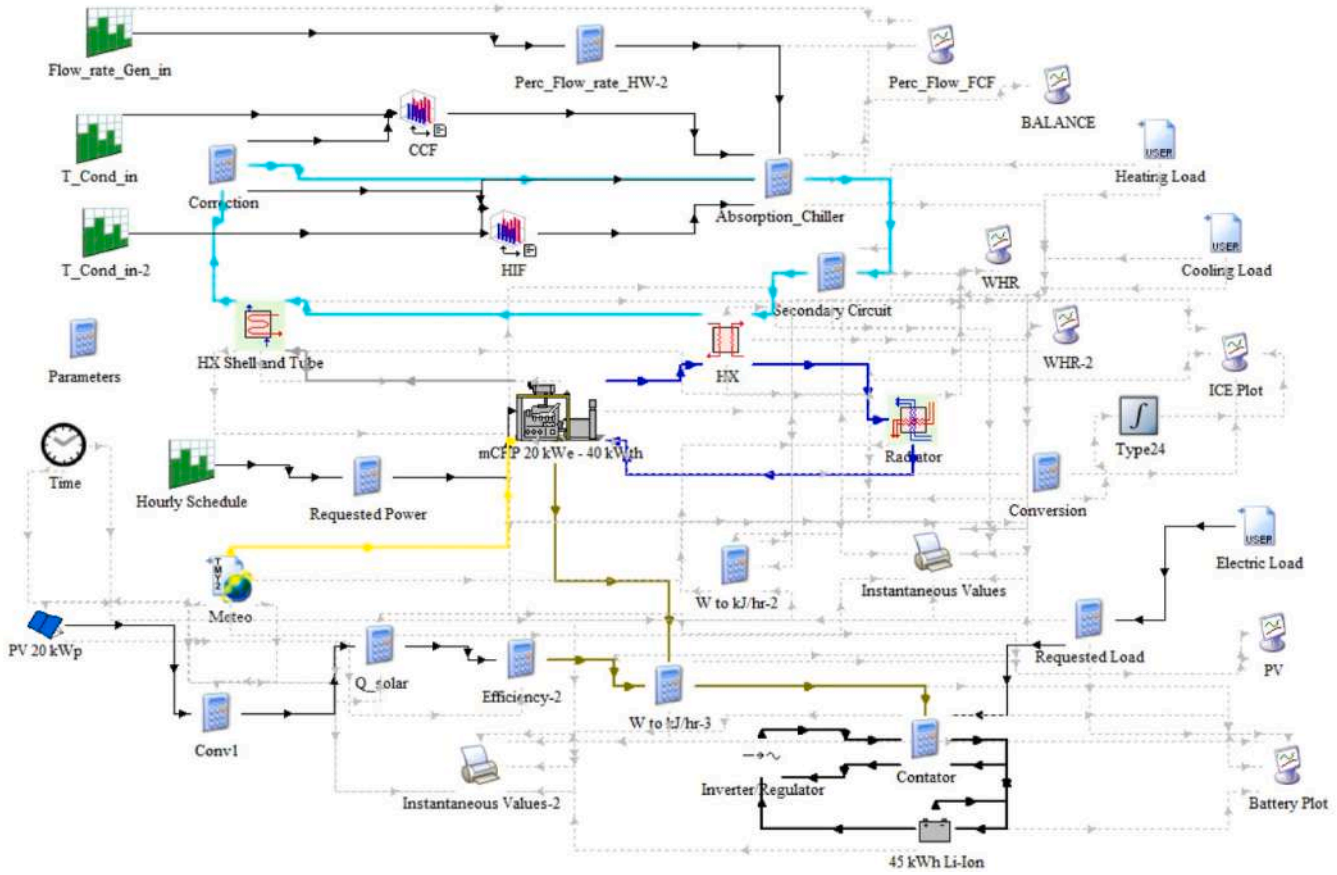

Fig. 9. Scheme of the proposed case study in TRNSYS environment.

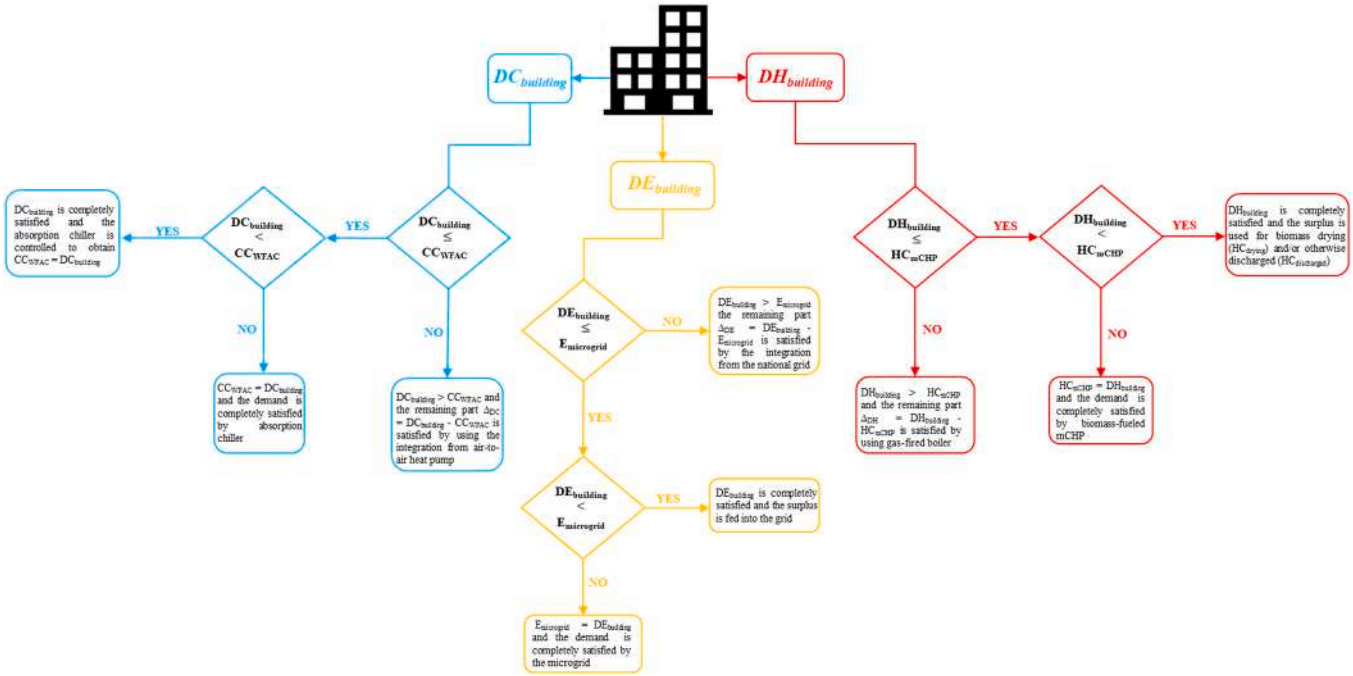

Fig. 10. Description of the control strategy of the microgrid.

3.1. *Description and motivation of the "PV-only" scenario*

To explain the benefits achievable by the combined use of RES in the framework of RECs, an additional system made up of only PV and a lithium battery (here briefly indicated as "PV-only") was assumed. The PV-only system was sized following the usual rules of thumb. More

Table 5
The scenarios assumed in the case study.

	P_z [€/MWh]	T_p [€/MWh]	T_{ARERA} [€/MWh]
SCENARIO 1 (S_1)	180	80	9.08
SCENARIO 2 (S_2)	160	100	
SCENARIO 3 (S_3)	140	120	
SCENARIO 4 (S_4)	100	120	
SCENARIO 5 (S_5)	60	120	

specifically, the sizing of the PV system and the energy storage system was carried out based on the annual electricity consumption of the user, amounting to 179,777.74 kWh/year. To determine the power of the photovoltaic system, a methodology based on the annual energy balance was adopted. Considering a specific yield of the system assumed to be 1600 kWh/kW$_p$ (a typical value for Southern Italy) [55], a nominal photovoltaic system capacity of approximately 110 kW$_p$ is required. Regarding the battery sizing, the criterion chosen was based on the adapted approach proposed in Ref. [56], where the battery capacity was evaluated according to the average daily energy used, the battery efficiency and the number of autonomous days for which the battery operation is required. In this work, the user's daily energy demand was approximately 492.54 kWh, the overall conversion chain efficiency (including inverter, controller, and battery) was 78.4 %, and the number of autonomous days was assumed equal to 1, because the PV-battery systems describe an operating mode in which the battery completes a charge and discharge cycle every day (daily-cycling strategy). The required nominal storage capacity, around 220 kWh, was calculated assuming that 35 % of the user's daily energy demand must be covered during early and late evening hours through previously stored energy. Subsequently, the performance of the sized "PV-only" system was evaluated through annual simulations, with a focus on two representative days: one in winter (January 22nd) and one in summer (June 30th). The simulation showed that PV generation typically reaches its maximum around midday, following the diurnal solar irradiance profile, whereas electricity demand generally peaks in the early morning and evening hours. Accordingly, the energy storage system provides temporal energy shifting from periods of surplus generation to those of higher demand, thereby enhancing the self-consumption of locally generated electricity [57].

Details on the simulation performed in TRNSYS and the associated scheme are provided in the Supplementary Material.

3.2. Description of the indicators

To quantify the energy, environmental, and economic benefits arising from the proposed systems, ad hoc indicators were used.

3.2.1. Energy indicators

To assess the self-sufficiency enabled by the PV-Biomass mCHCP system, the following indicators were defined over the time range t = 0–8760 h, in accordance with the plant management schedule and the criteria outlined in Section no. 2 (for the sake of clarity, please refer to Fig. 2): (i) I_{PSC} (see Eq. (9)) is the *Physical Self-Consumption index*, calculated by dividing the energy produced by the RES plant and consumed on-site (i.e., $Ec_€$), and the total amount of energy produced by the RES plant (E_P); (ii) I_{VSC} (see Eq. (10)) is the *Virtual Self-Consumption index*, determined by dividing the energy shared ($Es_€$) by the total energy produced; (iii) I_{TSC} is the *Total Self-Consumption index* obtained by summing the physical and virtual self-consumption indexes (see Eq. (11)); and (iv) I_{ESS} (see Eq. (12)) is the *Annual Energy Self-Sufficiency* index, calculated as the ratio between the energy produced on-site, shared, and self-consumed, and the total energy demand of the building (including energy required by each thermal zone $E_{u\,tot}$, as well as energy used for elevators, lighting, and equipment in the condominium's common areas E_C).

$$I_{PSC}\,[\%] = \frac{\sum_{t=0}^{8760} Ec_€}{\sum_{t=0}^{8760} E_p} \tag{9}$$

$$I_{VSC}[\%] = \frac{\sum_{t=0}^{8760} Es_€}{\sum_{t=0}^{8760} E_p} \tag{10}$$

$$I_{TSC}[\%] = I_{PSC} + I_{VSC} \tag{11}$$

$$I_{ESS}[\%] = \frac{\sum_{t=0}^{8760} (Es_€ + Ec_€)}{\sum_{t=0}^{8760} (E_{u\,tot} + E_C)} \tag{12}$$

To quantify the fraction of the thermal and cooling demands (i.e., $DH_{building}$ and $DC_{building}$) covered by the microgrid through the mCHP plant and WFAC, the following indicators were adopted: (i) I_{DH} (see Eq. (13)) is the fraction of the thermal demand of the building (from January to May, and from November to December) covered by the thermal energy from the mCHP (i.e., HC_{mCHP}); (ii) I_{DC} (see Eq. (14)) is the fraction of the cooling demand (from May to October) met by the cooling from the WFAC (CC_{WFAC}); and I_{TSS} is the annual thermal self-sufficiency index (see Eq. (15)).

$$I_{DH}\,[\%] = \frac{\sum_{t=0}^{8760} HC_{mCHP}}{\sum_{t=0}^{8760} DH_{building}} \tag{13}$$

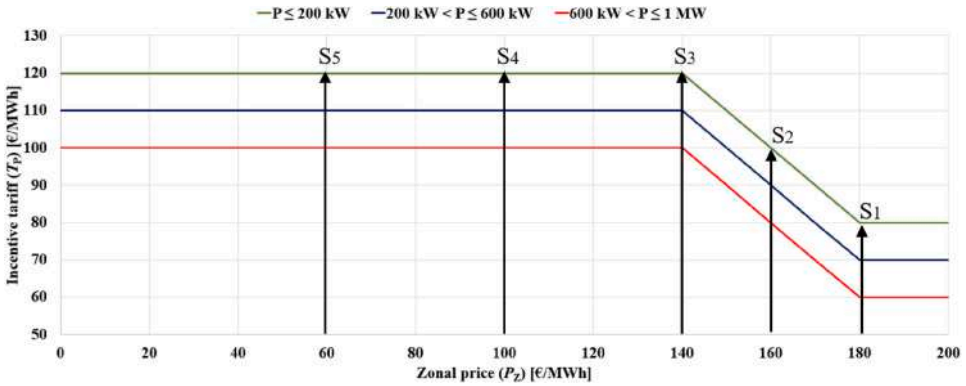

Fig. 11. Variation of incentive tariff with zonal price for the scenarios proposed.

$$I_{DC}\,[\%] = \frac{\sum_{t=0}^{8760} CC_{WFAC}}{\sum_{t=0}^{8760} DC_{building}} \tag{14}$$

$$I_{TSS}[\%] = \frac{\sum_{t=0}^{8760} HC_{mCHP} + \sum_{t=0}^{8760} CC_{WFAC}}{\sum_{t=0}^{8760} DH_{building} + \sum_{t=0}^{8760} DC_{building}} \tag{15}$$

Finally, as shown in Eqs (16) and (17), two further indicators were introduced to quantify the percentage of the yearly thermal energy produced by the PV-Biomass mCHCP plant which is usefully exploited by the users (I_{th_used} [%]) and the one which is finally dissipated ($I_{th\_discharged}$)

$$I_{th\_used}\,[\%] = \frac{\sum_{t=0}^{8760} HC_{mCHP} + \sum_{t=0}^{8760} CC_{WFAC} + \sum_{t=0}^{8760} HC_{drying}}{\sum_{t=0}^{8760} E_{th}} \tag{16}$$

$$I_{th\_discharged}\,[\%] = 1 - I_{th\_used} \tag{17}$$

In Eq. (16), E_{th} is the thermal energy yearly produced by the PV-Biomass mCHCP.

3.2.2. Economic and environmental indicators

The following economic indicators were included: Life Cycle Cost Saving (LCS), defined as the present value of the total energy cost savings over the lifetime, the Payback Time (PBT) and the Profitability Index (PI) evaluated considering the Net Present Value (NPV) (see Eqs. (22)–(24)). The investment cost C_0 equal to 290.32 k€ was calculated as the sum of the PV costs 0.95 k€/kW$_e$ [53], the mCHP cost 10 k€/kW$_e$ [42], the battery costs 1.3 k€/kWh$_e$ [52] and the WFAC cost 0.728 k€/kW$_f$ [48,58]. The annual benefits B_{net} were calculated as the difference between the revenues from incentives (energy shared, self-consumed and delivered in the grid), thermal (heating) and electric (cooling) energy saved with respect to the *base case* and the $C_{O\&M}$.

Regarding the energy saved evaluated for B_{net}, the natural gas was purchased to be used in a gas-fired for the $DH_{building}$ (heating season), electricity was taken from the grid to match the $DE_{building}$: a) for lighting, equipment from zones and common areas of the condominium, b) for air-to-air heat pumps for the $DC_{building}$ (only in cooling season). The operation and maintenance cost $C_{O\&M}$ equal to 28.17 k€ was calculated as the sum of 0.155 €/(kWh$_e$ y) for mCHP [42] also evaluated considering biomass cost equal to 100 €/ton$_{bio}$ (woodchip) purchased from the market, 15 €/(kW$_e$ y) for PV [53] and 274.56 €/y (assumed as 2 % of investment cost) for the WFAC [58]. The $C_{O\&M}$ of the battery is neglected. Also, 2 k€/y for GSE administrative practices on the Collective Self-Consumption incentive scheme realised by technicians, was considered. It regards drafting of the necessary, mandatory or required documentation, assistance on access and communication/consultation activities of the GSE.

These economic and environmental indicators were evaluated based on equations proposed by Refs. [53,59], duly adapted for the case study, as shown in the following:

$$B_{net}\,[k€/y] = B_{incentive} + B_{avoid\ ng} + B_{avoid\ el\ HP} - C_{O\&M} \tag{18}$$

$$B_{incentive}[k€/y] = En_{€}.P_Z + Es_{€}.T_p + Es_{€}.T_{ARERA} + Ec_{€}.C_{el} \tag{19}$$

$$B_{avoid\ ng} = \left[\frac{\left(\sum_{t=0}^{8760} HC_{mCHP}\right)}{\eta_{boil}}\right] \cdot C_{ng} \tag{20}$$

$$B_{avoid\ el\ HP} = \left[\frac{\sum_{t=0}^{8760} CC_{WFAC}}{\sum_{t=0}^{8760} EER_t}\right] \cdot C_{el} \tag{21}$$

$$LCS\,[k€] = \left[\frac{B_{net}}{(d - i_f)}\right] \cdot \left[1 - \left(\frac{1+i_f}{1+d}\right)^n\right] - C_0 \tag{22}$$

$$PBT\,[y] = \frac{ln\left[1 + \frac{C_0 \cdot (i_f - d)}{B_{net}}\right]}{ln\left(\frac{1+i_f}{1+d}\right)} \tag{23}$$

$$PI = \frac{NPV}{C_0} \tag{24}$$

The environmental performance of the proposed system was evaluated in terms of Reduction in CO_2 Emission (ER_{tot}) with respect to the *base case*, achieved thanks to the avoided natural gas used in gas-fired boiler (ER_{ng}) and avoided electrical demand by lighting, equipment and heat pumps (ER_{el}). Lastly, the total Environmental Penalty Cost Saving (EPCS), over the microgrid lifetime due to the reduction of carbon emissions was computed.

$$ER_{tot}[ton_{CO2}/y] = \sum_{t=0}^{8760} ER_{ng} + \sum_{t=0}^{8760} ER_{el} =$$

$$= \left[\sum_{t=0}^{8760}\left(\frac{HC_{mCHP}}{\eta_{boil}}\right)\right] \cdot f_{ng} + \left[\sum_{t=0}^{8760}(Es_{€} + Ec_{€})\right] \cdot f_{el} \tag{25}$$

$$EPCS\,[k€] = \left[\frac{ER_{tot} \cdot C_{CO2}}{(d - i_f)}\right] \cdot \left[1 - \left(\frac{1+i_f}{1+d}\right)^n\right] \tag{26}$$

The following values were assumed: market discount rate d equal to 8.0 %; fuel inflation rate i_f equal to 7.0 % [59]; electricity purchasing price with all taxes and levies included C_{el} equal to 0.334 €/kWh$_e$ [60]; natural gas price with all taxes and levies included C_{ng} equal to 0.134 €/kWh$_{th}$ [61]; plant lifetime of 20 years; CO_2 emission factor of natural gas f_{ng} equal to 0.206 kg$_{CO2}$/kWh$_{th}$ [53,62,63]; electricity emission factor f_{el} equal to 0.35 kg$_{CO2}$/kWh$_e$ [53,62,63]; and unit cost of CO_2 emission C_{CO2} equal to 0.07 €/kg$_{CO2}$ [53]. Emission factors represent the amount of CO_2 released per unit of electricity generated or fuel consumed (e.g., gCO$_2$/kWh, tCO$_2$/MWh, or tCO$_2$/TJ). Emission factors vary depending on several parameters, including fuel type and quality, as these determine the chemical composition and carbon content that ultimately influence pollutant emissions [64]. In this study, national emission factors are adopted as a key parameter for estimating the CO_2 emissions avoided through energy efficiency measures or reductions in electricity consumption. At the end-user level, the emission factor quantifies the amount of CO_2 avoided per kilowatt-hour of electricity not consumed, thereby reflecting the average carbon intensity of the national electricity mix. Conversely, at the generation level, substituting 1 kW-hour of electricity produced from fossil fuels with an equivalent amount generated from renewable sources results in the avoidance of CO_2 emissions corresponding to the respective emission factor. These data provide a consistent and comparable basis for the evaluation of different energy efficiency interventions and technologies within the electricity sector [63]. For Italy, baseline emission factors are published by national institutions such as TERNA (the Italian Transmission System Operator) and ISPRA (the Italian Institute for Environmental Protection and Research).

4. Results and discussion

Dynamic analyses were performed over a year, with energy results

available on an hourly and monthly basis. To gain deeper insight into the system's operation, a preliminary analysis of daily results is presented. In this respect, Fig. 12a-b shows the electrical energy exchanged on two typical days: one in winter (January 22nd) and one in summer (June 30th).

Fig. 12a shows that, in winter, from 00:00 to 07:00, the electricity produced by the mCHP (solid red line) is greater than user demand (dashed black line), with a consequent charging of the battery, as testified by the increasing SoC (solid blue line) and selling of electricity to the grid (solid green line). However, at 07:00, as the electricity demand of the user increases (becoming greater than the one available from mCHP), the battery begins to discharge, resulting in a reduction of SoC. However, no electricity is required from the grid. From 10:00 to 17:00, the electric power from the mCHP and PV (solid red line) exceeds the hourly electricity demand of the user, resulting in electricity being stored in the battery (solid gold line). Once the SoC of the battery (solid light blue line) reaches its maximum, the excess electricity (solid green line) is exported to the grid (solid green line). A similar trend is observed from 12:00 to 15:00. From 19:00 to 22:00, when the electricity demand of the user increases significantly, thus requiring additional power from the grid (dashed gold line). Moreover, the SoC of the battery reaches the minimum value (5 %) at around 21:30.

Fig. 12b illustrates electric power exchange in the summer day when the prime mover of the mCHP is offline for maintenance from 08:00 to 16:00. In this time, electricity demand is solely met by the PV system, leading to energy exchange with the battery and the power grid. In other hours, a similar trend to the one of the typical winter day could be observed.

Fig. 13a-b illustrates the energy flows exchanged during the weeks corresponding to the two selected typical days in winter (Fig. 13a) and in summer (Fig. 13b). In both figures the reference day was highlighted by light orange boxes. A similar pattern was observed for all day in the week. Again, the results indicate that the building requires grid integration, particularly in the evening hours when PV is not more available (dashed gold line) and the battery's SoC is at the minimum value, leaving the mCHP as the sole energy source. Again, the profiles point out the key role of the biomass in mitigating the variability and intermittency associated with non-programmable PV, especially in early and late evening and during nighttime, leading to lower discharge of the battery.

Fig. 14a shows the weekly profile of the thermal energy available from the prime mover (solid red line) and the heating demand of the user (dashed green line) during the winter. The energy available from the mCHP is typically greater than the demand of the user, except for a few hours where energy by the gas-fired boiler (dashed blue line) is required.

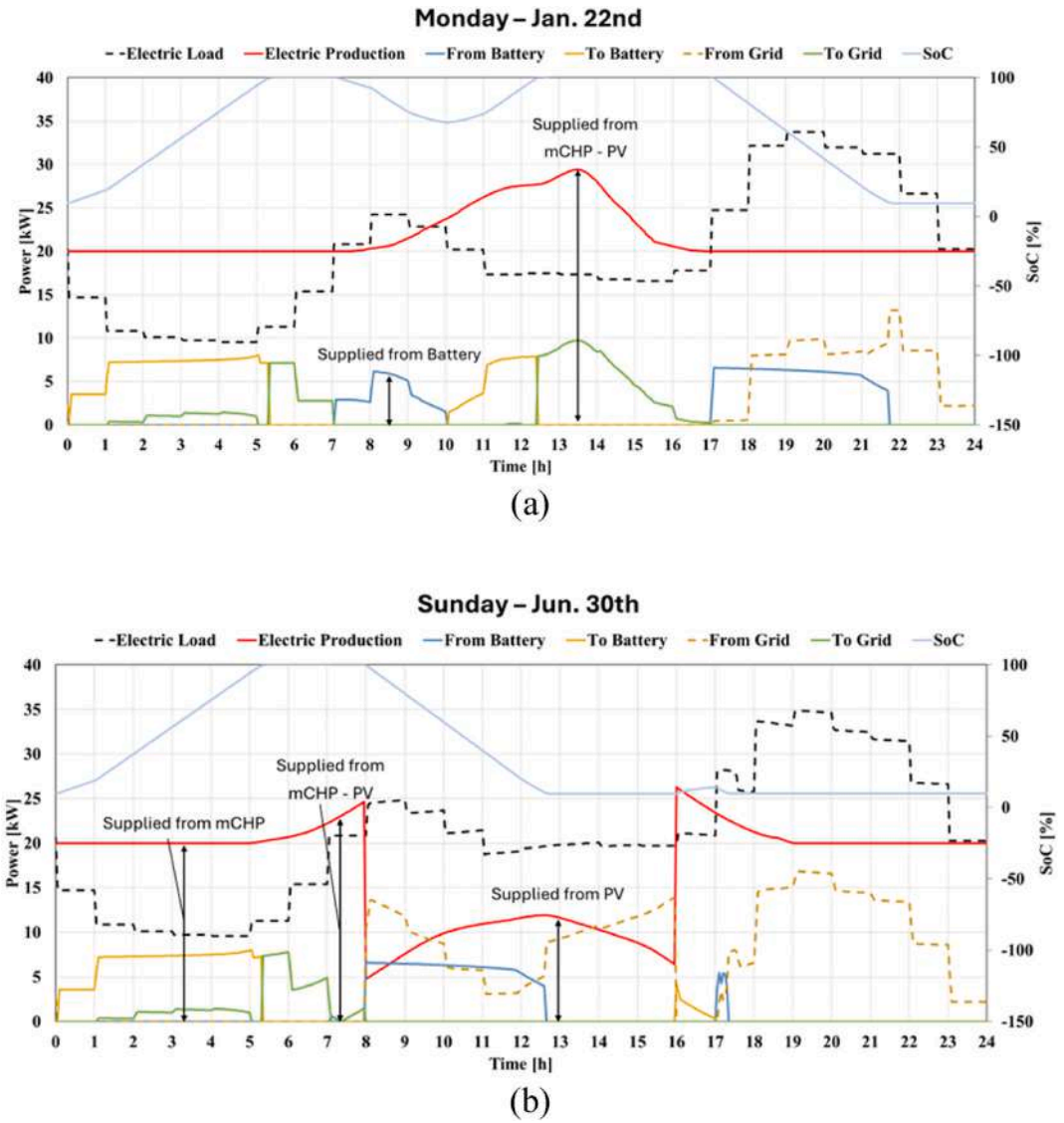

Fig. 12. Electric power flows in reference days: a) January 22nd, b) June 30th.

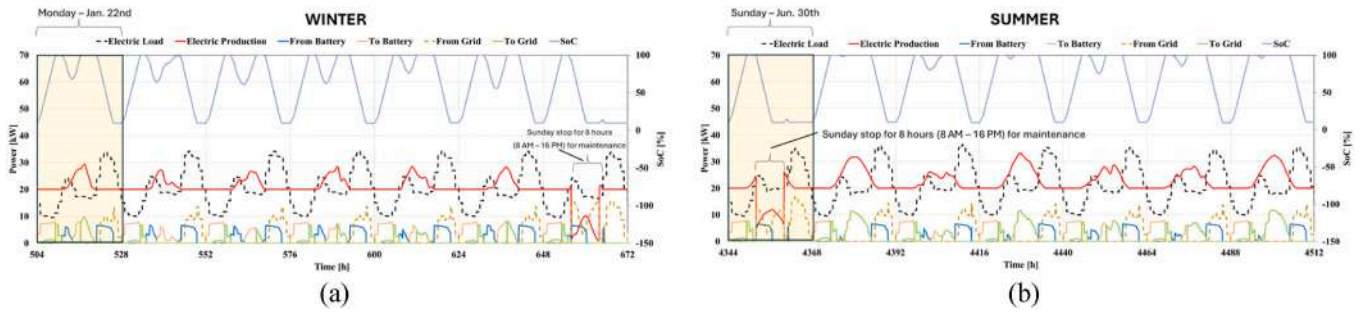

Fig. 13. Electric power flows in a reference week: a) in January, b) in June.

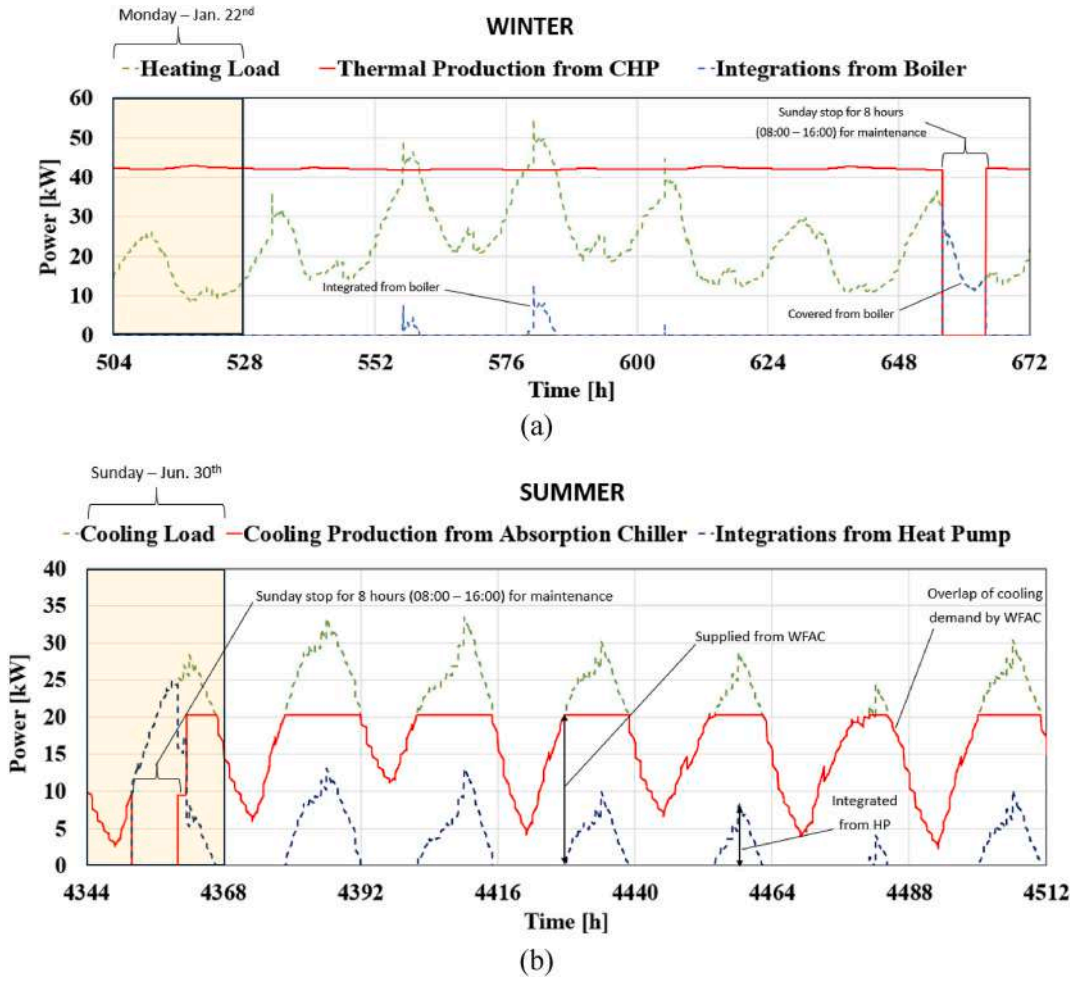

Fig. 14. Thermal and cooling power profile: a) reference week of January, and, b) referred to a week of June.

On Sunday when the ICE is off due to maintenance, the heating demand is entirely met by the boiler. In summer, Fig. 14b, as regards the cooling season, the WFAC partially covers the demand (solid red line vs dashed green one), and the building requires integrations from the splits systems (dashed blue line).

4.1. Analysis of the yearly energy results

Moving to yearly energy results, as shown in Fig. 15, the microgrid ensures a highly shared energy ($Es_{€}$, dashed purple bar) and physical self-consumption energy ($Ec_{€}$, dashed blue bar) compared to the electrical energy withdrawn from the zones (i.e., $E_{u\ tot}$, blue bars) and the energy consumed for common areas E_c (green bar). In particular, $Es_{€}$ accounts for 83.30 % of $E_{u\ tot}$, in August, and about 87.15 % in May. These suggest that the capability of the system to meet a large fraction of the electricity demand of the user. In addition, $Ec_{€}$ is equal to 99.12 % of E_c in December, and 100 % from May to August. It follows that the electricity required by the common areas is fully met by the energy produced by the RES plant.

As shown in Fig. 16, the PV-Biomass mCHCP system (see orange bars) meets approximately 92.95 % of the building's heating demand in January, increasing to 100 % in May. In summer, it covers via WFAC between 77.48 % in July and 96.04 % in October.

Considering the total thermal energy produced by the mCHP, 59.97 % was utilized to meet the building's thermal demand in January, 21.58 % for biomass pre-treatment, and 18.45 % was dissipated. In August,

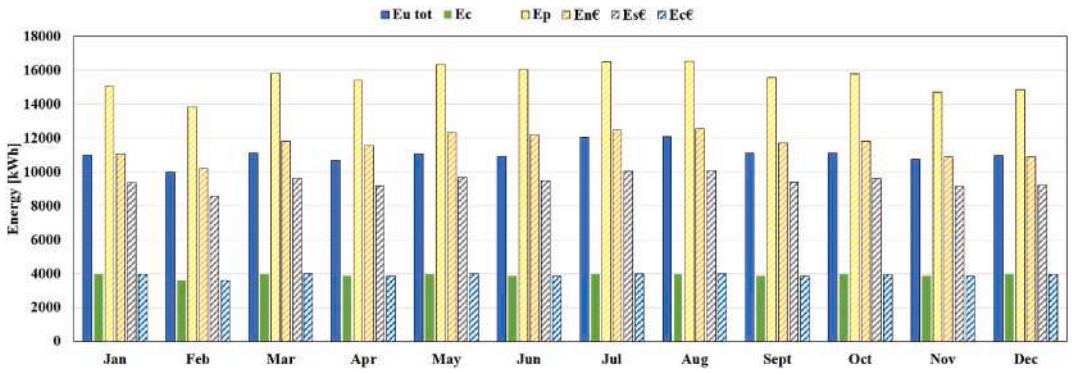

Fig. 15. Electrical energy exchanged on monthly basis.

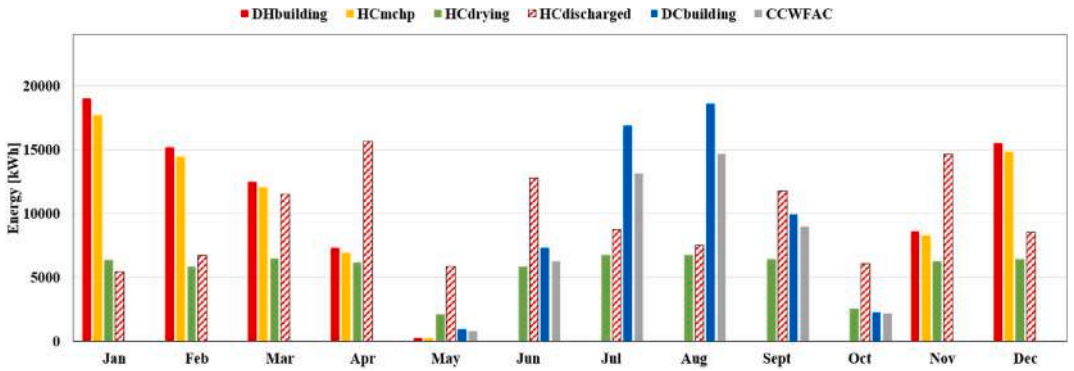

Fig. 16. Monthly heating and cooling energy comparison.

50.70 % was supplied to the WFAC to meet the building's cooling demand, 23.37 % was used for drying, and 25.93 % was dissipated. During the transitional season (e.g., April), 24.19 % of the thermal energy met the heating demand, 21.45 % was allocated to pre-treatment, and the dissipated portion rose to 54.36 %.

From yearly results, the energy indicators were then calculated. It was found that the physical self-consumption index I_{PSC} and the virtual self-consumption index I_{VSC} were equal to 25.2 % and 60.8 %, respectively. By comparing these results, it can be understood that the energy from the RES plant is mainly shared and used meeting the demand of the zones (almost 61 %), with 25.2 % physically consumed for meeting the electricity demand of common areas. In addition, the total self-consumption index I_{TSC} is equal to 86.0 %, suggesting that almost a small fraction of the electricity from RES is exported to the grid. The energy self-sufficiency index I_{ESS} is 89.1 %, indicating that the proposed system allows to cover a large fraction of the demand of the reference building.

Regarding the annual thermal covered demand index I_{DH}, the annual cooling covered demand index I_{DC} and the annual thermal self-sufficiency index I_{TSS}, are equal to 95.0 %, 74 % and 86.0 %, respectively. The amount of thermal energy recovered from the mCHP, which is usefully exploited by the building to cover its air-conditioning demand and biomass drying pre-treatment, (I_{th_used}) is equal to 62.05 %, being the 37.95 % wasted. This result is very promising, considering that (i) no thermal energy storage was included in the analysis, meaning that further energy savings could be achieved by properly sizing this component; (ii) the size of the mCHP has been selected by following a typical heuristic approach, without any optimization which can suggest; and (iii) the waste of thermal energy could be reduced in those context where a heat sharing is possible, with a further revenue for the CSC.

In conclusion, from an environmental point of view, a total emissions reduction (ER_{tot}) of 74.81 tons CO_2/year (−90.5 %) was found with respect to the base case, with electrical emissions reduction (ER_{el}) and natural gas emissions reduction (ER_{ng}) equal to 56.08 tons CO_2/year (−89.1 %) and 18.73 tons CO_2/year (−95 %), respectively. An Environmental Penalty Cost Saving (*EPCS*) of 88.90 k€ was found.

4.2. *Effects of incentive tariff on revenues and feasibility of the investment*

Fig. 17a-d shows the monetary flows in the reference weeks for the following scenarios: S_1 (Fig. 17a–b) and S_5 (Fig. 17c–d). As shown in Fig. 17a, in the S_1 scenario, the $B_{incentive}$ (solid red line) is primarily influenced by the sale of excess electricity to the grid.

$En_€$ (solid blue line) in winter and in summer, followed by revenues from self-consumed electricity in common areas $Ec_€$ (solid yellow line), and revenues from shared energy $Es_€$ (solid orange line). Moreover, the contribution from avoided transmission losses (grey line) is negligible. A similar hierarchy is observed in summer (see Fig. 17b), although the $B_{incentive}$ is higher due to increased net electricity production from RES plants and higher feed-in to the grid, attributed to greater solar radiation. In contrast, in scenario S_5, the lower zonal price results in a reduction of the $B_{incentive}$. In this case Fig. 17c-d, unlike S_1, revenues from net electricity fed into the grid by RES plants (solid blue line) become lower than those from shared energy. Moreover, although lower zonal prices lead to an increase in T_p (see Table 5), the higher incentive tariff is not sufficient to offset the reduced revenues from surplus electricity sales, ultimately resulting in a lower $B_{incentive}$.

Moving to annual results (see Table 6), the analysis reveals a slight variation in revenues from incentives $B_{incentive}$ (consisting of energy shared, self-consumed and delivered to the grid) from S_1 to S_3: 1.03 % for S_2 and -2.05 % for S_3 compared to S1, being the PBT and PI approximately constant. Instead, moving from S_4 to S_5: 13.03 % for S_4 and -24.0 % for S_5 reduction in $B_{incentive}$ is observed, and PBT becomes greater than 10 years, due to the saturation of T_p. The corresponding PIs remain below unity.

Two critical issues can then be identified. For a system of this kind,

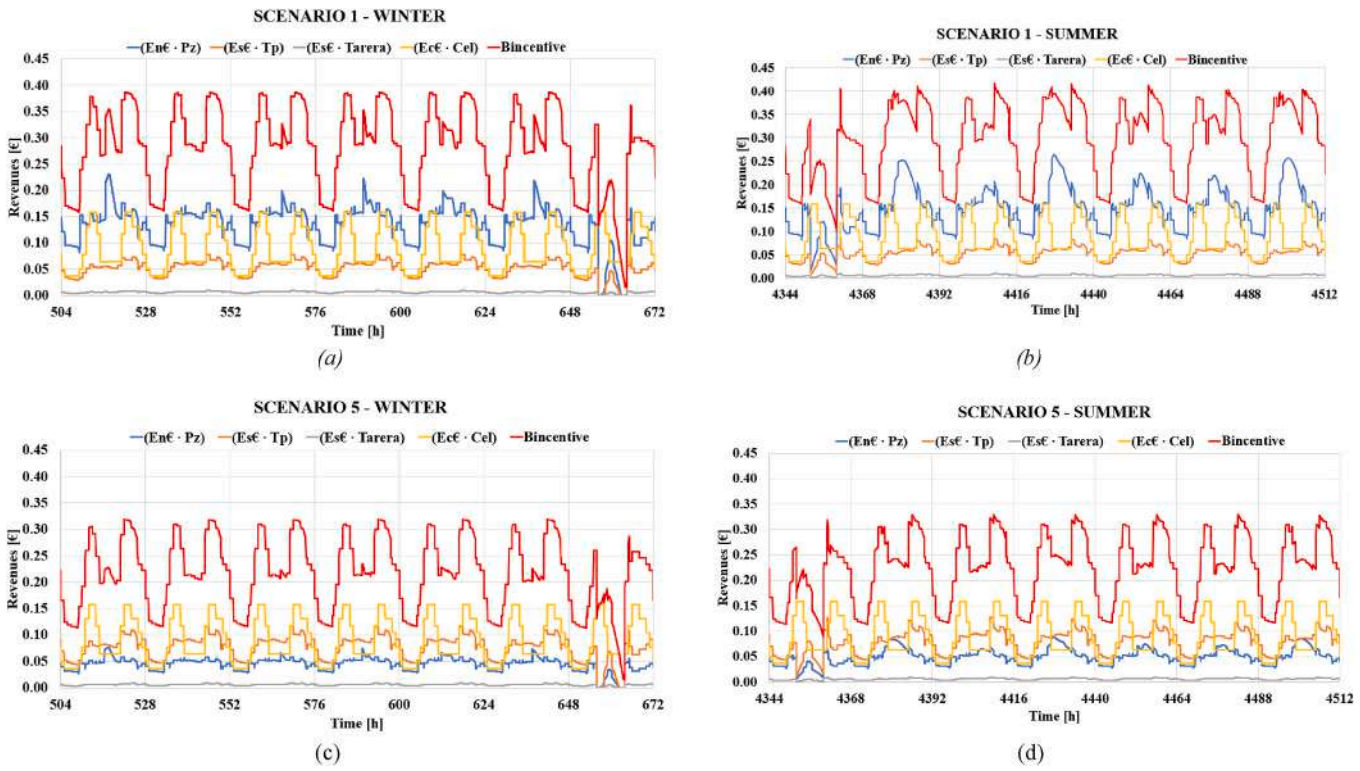

Fig. 17. Revenues from incentives: referred to a week of January in winter a) for the best scenario (S_1) and b) for the worst case (S_5), referred to a week of June in summer c) for the best scenario (S_1) and d) for the worst case (S_5).

Table 6
Economic analysis for the examined scenarios.

	$B_{incentive}$[€/y]	B_{net} [€/y]	LCS [k€]	PBT [y]	PI [−]
SCENARIO 1 (S_1)	50859.07	37324.28	343.32	8.70	1.18
SCENARIO 2 (S_2)	50336.76	36801.97	334.45	8.83	1.15
SCENARIO 3 (S_3)	49814.44	36279.65	325.59	8.97	1.12
SCENARIO 4 (S_4)	44234.03	30699.24	230.85	10.68	0.80
SCENARIO 5 (S_5)	38653.61	25118.82	136.11	13.20	0.47

linking the incentive to the zonal electricity price could be risky, as it would significantly reduce the $B_{incentive}$ and considerably extend the payback period. A decline in zonal prices is foreseeable due to the continuous growth of renewable energy sources within the electricity generation mix. Furthermore, it is proposed to index the T_p also to the CAPEX of the available renewable technologies, promote the integration of diverse energy sources within RECs.

4.3. Comparison of the proposed systems with the "PV-only" system

Results for the "PV-only" scenario for the reference weeks in winter (Fig. 18a) and summer (Fig. 18b) are shown. Additionally, results for two typical days, January 22nd and June 30th, are collected in the Supplementary Material.

By comparing these results with ones found for the reference PV-Biomass mCHCP system (Fig. 13a-b.), it is worth noting that.

- Especially in winter, the SoC of the battery never reaches the maximum value, with electricity stored mostly consumed at the end of the afternoon. Therefore, the user must rely on the power grid to meet its demand during early and late evening hours and the nighttime (see the overlap between the dashed gold and black lines) since no electricity is available from the battery (neither from the PV-Biomass mCHCP plant).
- In comparison to the proposed system, the energy exchanged, whether shared, self-consumed, or delivered to the grid, remains very low and is strictly dependent on solar radiation and PV-battery system operation. As a result, revenues for the plant owner are significantly reduced.

On a yearly basis, it was found that the PV-battery system is capable to provide 68051.09 kWh, covering about 37.8 % of the electrical energy demanded by the user. Similar self-consumption percentages are shown in ref. [65] for a residential building. Meantime, about 83067.16 kWh can be sold to the grid. In Table 7 results from the economic analysis for the five scenarios are presented. Moreover, the percentage variation compared to the results found for the PV-Biomass mCHCP system (see Table 6) is shown. First, about 27–30 % reduction in the revenues from the incentive was found due to the lower amount of energy exchanged. However, the percentage variation in net revenues decreases to −4 %. The life cycle cost was decreased from 40 % to 70 %, although the PV-Biomass mCHCP system presents a higher upfront cost. Finally, a higher PBT is found for the case of the PV-only system. As shown in Table 7, the B_{net} value is only marginally reduced. This outcome is primarily due to the significantly lower O&M cost of the PV system, which amounts to 3650 €/year, approximately 7.71 times lower than that of the PV-Biomass mCHCP system (28,166.55 €/year).

4.4. Sensitivity analysis on biomass cost

As previously detailed, the total O&M costs of the PV-Biomass mCHCP system were evaluated at 28,166.55 €/year, where 91.83 % (25,866.56 €) is attributable to the Biomass mCHCP subsystem. This includes both direct maintenance expenditures (27.06 %) and the annual cost of biomass supply (72.94 %), evaluated considering biomass cost equal to 100 €/ton_{bio} (woodchip). Appears clear that the profitability of the PV-Biomass mCHCP system depends on the price of wood chips, which varies considerably with the biomass quality. The price is

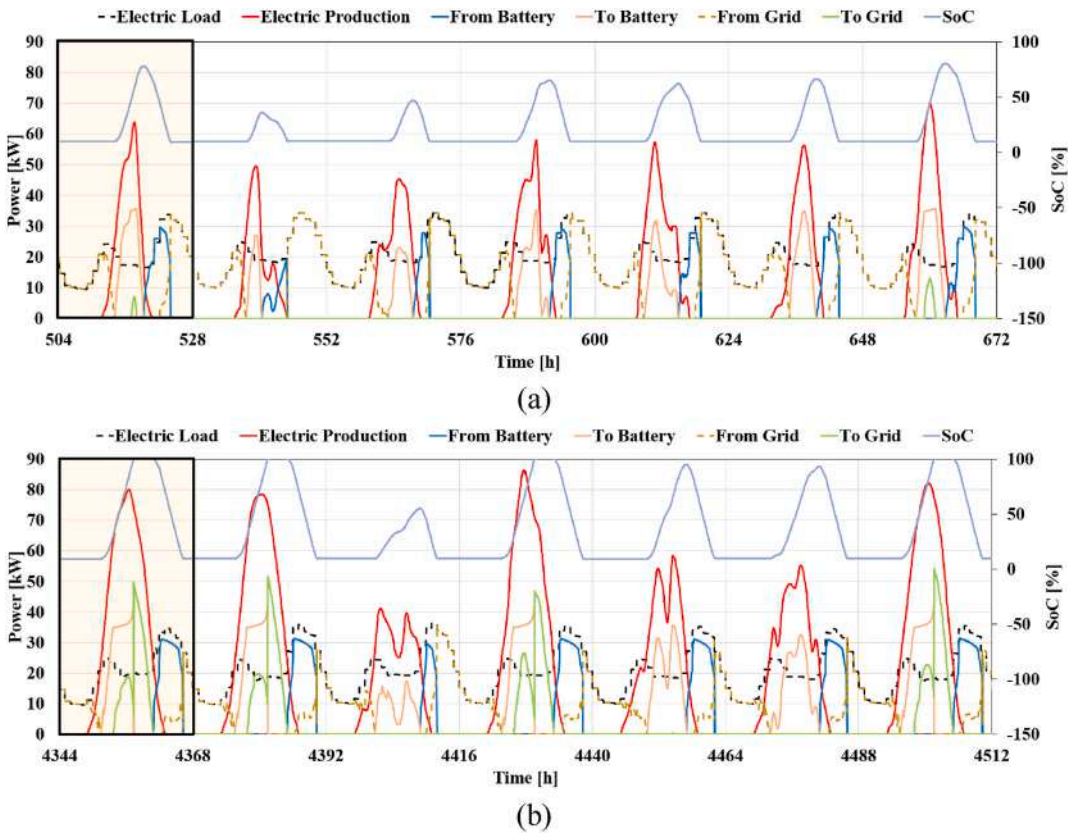

Fig. 18. Electric power flow for the "only-PV" scenario: a) winter week, and b) summer week.

Table 7
Economic analysis for the "PV-only" scenario.

	$B_{incentive}$[€/y]	$\Delta B_{incentive}$[%]	B_{net} [€/y]	ΔB_{net} [%]	LCS [k€]	ΔLCS [%]	PBT [y]	ΔPBT [y]
SCENARIO 1 (S_1)	37019.82	−27.2 %	35820.56	−4.0 %	204.79	−40.4 %	12.84	+4.14
SCENARIO 2 (S_2)	36303.44	−27.9 %	35104.18	−4.6 %	192.63	−42.4 %	13.12	+4.29
SCENARIO 3 (S_3)	35587.07	−28.6 %	34387.8	−5.2 %	180.47	−44.6 %	13.41	+4.44
SCENARIO 4 (S_4)	31187.34	−29.5 %	29988.08	−2.3 %	105.78	−54.2 %	15.53	+4.85
SCENARIO 5 (S_5)	26787.62	−30.7 %	25588.35	1.9 %	31.08	−77.2 %	18.44	+5.24

primarily determined by the moisture content, which can vary from dry material to significantly higher levels for wet biomass. Particle size uniformity also influences market value and depends on multiple factors, including the characteristics of the raw wood, the type and maintenance of the chipper, and any sieving processes applied [40]. Together, these parameters define chip quality and, consequently, its market price. Transportation costs further affect the final price [66], typically adding between 20 and 50 €/ton depending on the site, the delivery distance and the transport method used [67]. According to data reported by the Italian Agroforestry Energy Association (AIEL) [68], in September 2025, the average price for Class A1 chips, characterized by low moisture content (≤25 % w/w), high calorific value (≥13 MJ/kg) and low ash content (≤1 % w/w), was 136 €/ton with a slight decrease of 1 €/ton compared to September 2024, while remaining stable relative to April 2025. In contrast, Classes A2 and B1 recorded moderate price increases over the same period. Specifically, Class A2 experienced an 8 % rise, reaching 107 €/ton (equivalent to approximately 34 €/MWh), whereas Class B1, with high moisture contents up to 50 % w/w and low calorific value (≥8 MJ/kg), showed a smaller increase of 6 %, from 52 €/ton in September 2024 to 55 €/ton in September 2025 [67]. Based on these recent data, a sensitivity analysis on biomass cost was conducted, varying the price from 0 €/ton, when the biomass feedstock could be collected locally and supplied free of charge by community members, passing from 50 €/ton for Class B1 up to 180 €/ton for Class A1.

The first new scenario with a biomass price equal to 0 €/ton is plausible in RECs where stakeholders, such as agricultural cooperatives or forestry consortia, collect residual biomass from dead branches and prunings. Under this assumption, the mCHP-specific O&M cost would decrease significantly, from 0.155 €/(kWh_e·y), evaluated in the reference case with a maintenance cost of 7000 €/year and a biomass cost equal to 100 €/ton_{bio}, to 0.0466 €/(kWh_e·y). The total O&M costs of the PV-Biomass mCHCP would fall to 10,076.65 €/year (−64.22 %). Consequently, moving from S_1 to S_5, the B_{net} increases from +48.47 % to +72.02 %, the PBT decreases from 2.92 to 6.61 years, and the PI increases from +89.86 % to +224.82 %, compared to the scenario proposed in Table 6. Instead, considering the scenario shown in Table 7, the B_{net} increases from +54.70 % to +68.86 %, and PBT decreases from 7.06 to 10.86 years (Table 8).

In the worst-case scenario with a maximum value of 180 €/t, the mCHP-specific O&M cost would increase to 0.243 €/(kWh_e·y), and consequently, the total O&M costs of the PV-Biomass mCHCP rise to 42,852.08 €/year (+52.14 %). As detailed in Table 9, moving from S_1 to S_5, the B_{net} decreases from −39.35 % to −72.05 %, the PBT increases from 6.05 to 21.85 years, and the PI decreases from −72.56 % to −182.96 % compared to the scenario proposed in Table 6. Instead, considering the scenario shown in Table 7, the B_{net} also decreases from

Table 8
Economic analysis for the favourable scenarios (P_{bio} = 0 €/t).

	B_{net} [€/y]	PBT [y]	PI [−]	ΔB_{net} [%] (ref. Table 6)	ΔPBT [y] (ref. Table 6)	ΔPI [%] (ref. Table 6)	ΔB_{net} [%] (ref. Table 7)	ΔPBT [y] (ref. Table 7)
SCENARIO 1 (S_1)	55414.18	5.78	2.24	+48.47	−2.92	+89.86	+54.70	−7.06
SCENARIO 2 (S_2)	54891.87	5.84	2.21	+49.15	−2.99	+92.16	+56.37	−7.28
SCENARIO 3 (S_3)	54369.55	5.90	2.18	+49.86	−3.07	+94.58	+58.11	−7.51
SCENARIO 4 (S_4)	48789.14	6.59	1.85	+58.93	−3.20	+131.25	+62.70	−8.94
SCENARIO 5 (S_5)	43208.72	7.48	1.53	+72.02	−6.61	+224.82	+68.86	−10.96

Table 9
Economic analysis for the worst-case scenarios (P_{bio} = 180 €/t).

	B_{net} [€/y]	PBT [y]	PI [−]	ΔB_{net} [%] (ref. Table 6)	ΔPBT [y] (ref. Table 6)	ΔPI [%] (ref. Table 6)	ΔB_{net} [%] (ref. Table 7)	ΔPBT [y] (ref. Table 7)
SCENARIO 1 (S_1)	22638.76	14.75	0.32	−39.35	6.05	−72.56	−36.80	1.91
SCENARIO 2 (S_2)	22116.44	15.13	0.29	−40.75	6.30	−74.50	−38.26	2.01
SCENARIO 3 (S_3)	21594.13	15.52	0.26	−42.14	6.55	−76.54	−39.72	2.11
SCENARIO 4 (S_4)	16013.71	21.50	−0.06	−57.10	10.82	−107.50	−55.29	5.97
SCENARIO 5 (S_5)	10433.29	35.05	−0.39	−72.05	21.85	−182.96	−70.87	16.61

−36.80 % to −70.87 %, and PBT increases from 1.91 to 16.61 years.

Fig. 19 highlights the variation of the Life Cycle Cost Saving as a function of zonal price and biomass cost. These results are consistent with the findings discussed above, confirming the techno-economic viability of the proposed system in scenarios where biomass is available at negligible or zero cost. Conversely, the system's performance is significantly affected by rising biomass prices, becoming particularly unfavorable in contexts characterized by constrained zonal electricity

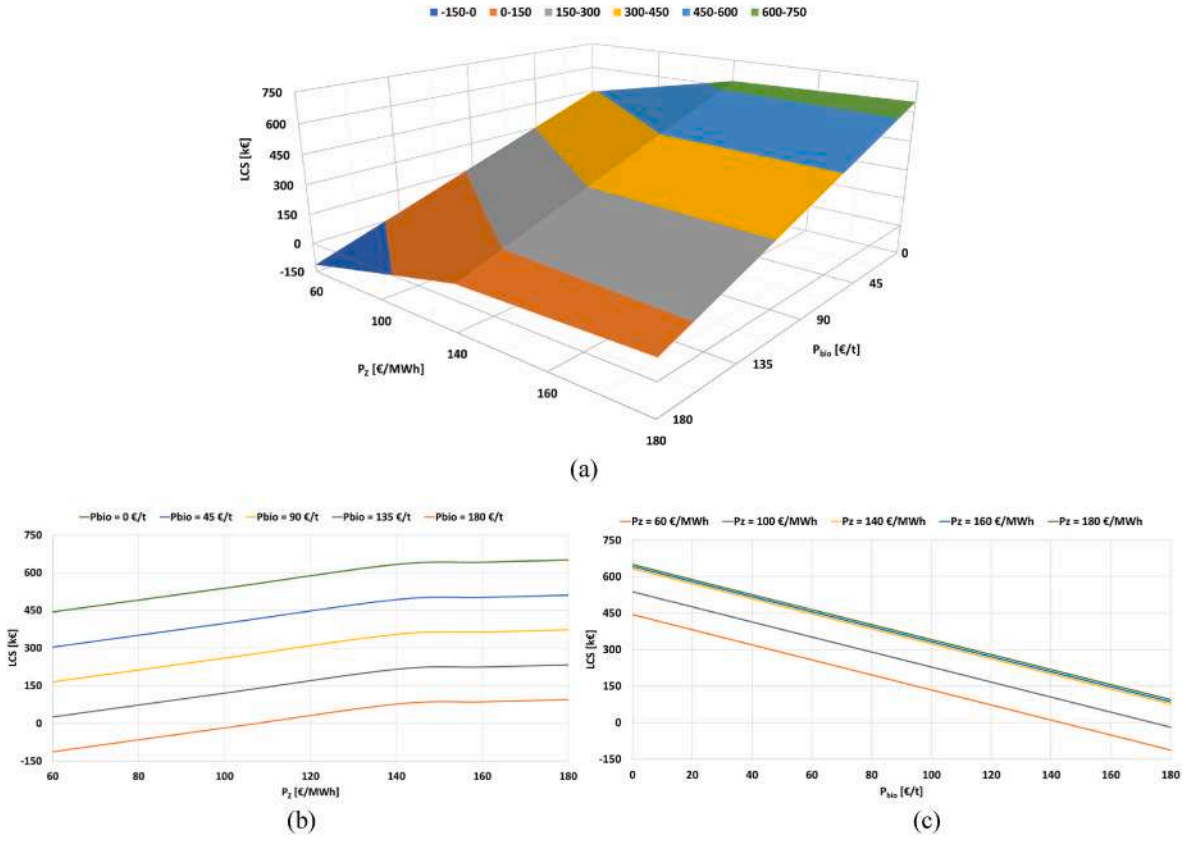

Fig. 19. Variation in LCS as a function of: a) zonal price and biomass cost, b) only zonal price, c) only biomass cost.

prices.

The adverse effects on investment profitability caused by the increase in biomass cost and the reduction in the zonal electricity price could be offset only through a substantial decrease in the microgrid capital cost, which currently represents a significant barrier to its practical deployment (Fig. 20). For instance, considering the initial investment cost C_0 equal to 290.32 k€ and assuming the worst-case with a fixed biomass price of 180 €/t, the limit scenario with $P_z = 60$ €/MWh (solid orange line, Fig. 20) achieves a PI greater than unity only if the initial investment cost is reduced by approximately 70 % ($C_0 = 87.09$ k€).

4.5. Limitations of the study and future remarks

Before ending it is worth mentioning the limitations of the present study, which constitute the basis for future analysis.

- The nominal capacity of each component (both the prime mover of the Biomass mCHCP plant, PVs and battery) was selected by using heuristic approaches, without relying on an optimization procedure. An optimization study should be then performed to enhance the energy and economic performance of this system under the available incentive framework, increasing the attractivity in the field. As part of future research developments, optimization-based dimensioning methods will be developed and tested.
- A simple operating strategy of the PV-Biomass mCHCP (full-load operation) was assumed, duly justified by the FLEC curve. However, more refined strategies should be investigated to better exploit the potential energy available from biomass, to account for the variability of boundary conditions such as zonal prices.
- The possibility of including a thermal energy storage for storing the thermal energy recovered from the mCHP should be investigated, thus leading to lower thermal energy waste. Moreover, the effect of operating these systems in the presence of district heating networks should be examined considering the renewed interest in this technology, where the possibility of selling excess heat to the network could lead to additional revenue for plant owners, decreasing the PBTs.
- The analysis investigated the feasibility of REC with the joint use of RESs in the current legislative framework without proposing a new one. For this reason, future studies should examine alternative financial strategies, while considering the effects of uncertainties in market electricity prices.

5. Conclusions

The work presents a 3E analysis of a PV-Biomass mCHCP system serving an apartment building in the case of CSC. Dynamic analyses on an hourly basis were performed in TRNSYS. The microgrid performances with the base case (gas-fired boiler used in the heating season and air-to-air HP used only in the cooling season) were compared from the energy, economic, and environmental points of view, also considering the incentive tariffs from the current regulatory framework in Italy on RECs. Results indicate that a PV-Biomass mCHCP system sized following a heuristic approach can cover a significant portion of the energy demand when appropriately sized to match the load requirements. In particular, in this study, the physical self-consumption index, the virtual self-consumption index, the total self-consumption index and the energy self-sufficiency index were equal to 25.2 %, 60.8 %, 86.0 % and 89.1 %, respectively. Instead, the annual thermal covered demand index, the annual cooling covered demand index, and the annual thermal self-sufficiency index were equal to 95.0 %, 74 %, and 86.0 %, respectively. In terms of environmental point of view, the microgrid can guarantee an Emission Reduction of CO_2 ER_{tot} of 74.81 ton $_{CO2}$/y (−90.5 %) with ER_{el} and ER_{ng} equal to 56.08 ton $_{CO2}$/y (−89.1 %) and 18.73 ton $_{CO2}$/y (−95 %), respectively and an Environmental Penalty Cost Saving *EPCS* of 88.90 k. A comparison with a PV-only system serving the same user under the CSC scheme leads to 4 % lower economic revenues, but PBT increases of about 4 years. However, the findings highlight the suitability of the proposed technology in contexts where biomass can be sourced at minimal or no cost, thereby significantly improving its economic viability. The analysis indicates that the high upfront costs associated with developing the proposed microgrid may hinder its implementation, despite its potential to valorize an otherwise wasted resource. Additionally, there is an urgent need for incentive mechanisms for RECs and CSCs tailored to available RES technologies.

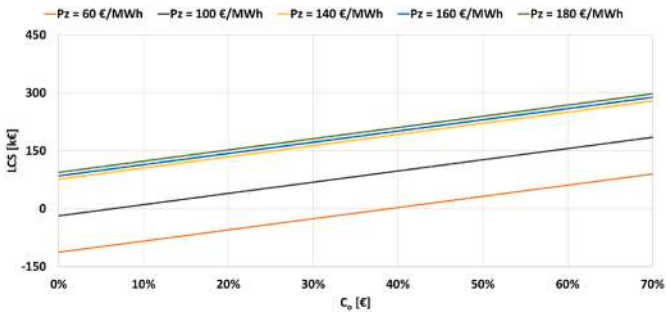

Fig. 20. Variation in LCS as a function of investment cost reduction (biomass cost fixed to 180 €/t).

CRediT authorship contribution statement

Maurizio La Villetta: Writing – review & editing, Writing – original draft, Visualization, Validation, Supervision, Software, Resources, Project administration, Methodology, Investigation, Funding acquisition, Formal analysis, Data curation, Conceptualization. **Daniele Piazzullo:** Writing – review & editing, Writing – original draft, Visualization, Validation, Supervision, Software, Resources, Project administration, Methodology, Investigation, Funding acquisition, Formal analysis, Data curation, Conceptualization. **Pietro Catrini:** Writing – review & editing, Writing – original draft, Visualization, Validation, Supervision, Software, Resources, Project administration, Methodology, Investigation, Funding acquisition, Formal analysis, Data curation, Conceptualization. **Antonio Piacentino:** Writing – review & editing, Writing – original draft, Visualization, Validation, Supervision, Software, Resources, Project administration, Methodology, Investigation, Funding acquisition, Formal analysis, Data curation, Conceptualization. **Michela Costa:** Writing – review & editing, Writing – original draft, Visualization, Validation, Supervision, Software, Resources, Project administration, Methodology, Investigation, Funding acquisition, Formal analysis, Data curation, Conceptualization.

Declaration of competing interest

The authors declare that they have no known competing financial interests or personal relationships that could have appeared to influence the work reported in this paper.

Acknowledgement

This study was developed in the framework of the research activities carried out within the Project “Network 4 Energy Sustainable Transition - NEST”, Spoke 7: Smart Sector Integration, Project code PE0000021, CUP: B73C22001280006, funded under the National Recovery and Resilience Plan (NRRP), Mission 4, Component 2, Investment 1.3 - Call for tender No. 1561 of October 11, 2022 of Ministero dell’Università e della Ricerca (MUR); funded by the European Union - NextGenerationEU.

Appendix A

Regarding the additional contribution due to avoided losses on the grid, T_{arera}, different remunerations are proposed according to energy shared under the same primary substation.

1. in the case of RECs and PSCs, the highest value of the tariff for the transmission service ($TRAS_E$), equal to 8.48 €/MWh in 2023, is considered.
2. in the case of CSCs, is considered the sum of:
   a) the highest value of the $TRAS_E$.
   b) the highest value of the tariff for low-voltage connections, equal to 0.6 €/MWh in 2023.
   c) the value of avoided losses, equal to the zonal price multiplied by the coefficient:
      – 1.2 % in the case of shared energy from generation plants connected to medium voltage.
      – 2.6 % in the case of energy shared by production plants connected to low voltage.

Appendix B. Supplementary data

Supplementary data to this article can be found online at https://doi.org/10.1016/j.energy.2025.139692.

Nomenclature

Acronyms/abbreviations	
AC	Alternating current
ATD	Aggregate Thermal Demand
CSC	Collective Self-Consumption
ECs	Energy Communities
DC	Direct current
EU	European Union
FLEC	Full Load Energy Curve
GSE	Gestore dei Servizi Energetici
HPs	Heat Pumps
ICE	Internal Combustion Engine
MASE	Minister of Environment and Energy Security
mCHP	Micro Combined Heat and Power
mCHCP	Micro Combined Heat, Cooling and Power
MISE	Minister of Economic Development
N	Nord (cardinal direction)
NRRP	National Recovery and Resilience Plan
O	Ovest (cardinal direction)
PSC	Personal Self-Consumption
POD	Point Of Delivery
PV	Photovoltaic system
RECs	Renewable Energy Communities
RED	Renewable Energy Directive
RES	Renewable Energy Systems
RSC	Renewable Self-Consumers
S	Sud (cardinal direction)
UK	United Kingdom
US	United States
TRNSYS	TRaNsient SYstems Simulation
W	West (cardinal direction)
WFAC	Water-fired absorption chiller
Variables	
$B_{avoid\ el\ HP}$	Revenues from electric energy saved (cooling) [k€/y]
$B_{avoid\ ng}$	Revenues from thermal energy saved (heating) [k€/y]
$B_{incentive}$	Revenues from incentivised (energy shared, self-consumed and delivered in the grid) [k€/y]
B_{net}	Annual benefits [k€/y]
BTAU	Tariff for low-voltage connections [€/kWh$_e$]
c_{el}	Electricity purchase [€/kWh$_e$]
c_{ng}	Natural gas price [€/kWh$_{th}$]
C_0	Capital cost [k€]
C_{CO2}	Cost of unit CO_2 emission [€/kg$_{CO2}$]
$C_{O\&M}$	Operation and maintenance cost [k€/y]
CC_{WFAC}	Cooling capacity from WFAC [kW$_f$] or Cooling demand from building covered by WFAC [kW$_f$]
CCF	Cooling Capacity Factor [−]
COP_{WFAC}	Coefficient Of Performance of the water-fired absorption chiller
d	Market discount rate [%]
$DC_{building}$	Cooling demand from building [kW$_f$]
$DE_{building}$	Electricity demand from building [kW$_e$]
$DH_{building}$	Heating demand from building [kW$_{th}$]
$E_{microgrid}$	Electricity demand from building covered by microgrid [kW$_e$]
Ec	Real energy consumed from elevator, lighting and equipment from corridor zones of condominium [kWh$_e$]
Ec_{ϵ}	Physical self-consumption energy consumed [kWh$_e$]
En_{ϵ}	Net electrical energy produced and fed into the grid by the RES plants [kWh$_e$]
E_P	Total energy produced by RES [kWh$_e$]

(*continued on next page*)

(*continued*)

$E_{PV\text{-}only}$	PV + lithium battery production [kWh_e]
EPCS	Environmental penalty cost saving [k€]
ER_{el}	Emission reduction of CO_2 from avoided electrical demand from lighting, equipment and heat pump taken from the national grid [ton_{CO2}/y]
ER_{ng}	Emission reduction of CO_2 from avoided natural used in gas-fired boiler [ton_{CO2}/y]
ER_{tot}	Total Emission Reduction of CO_2 [ton_{CO2}/y]
$Es_€$	Shared energy [kWh]
E_{ui}	Electrical energy withdrawn from the single zone [kWh_e]
$E_{u\ tot}$	Electrical energy withdrawn from the zones [kWh_e]
EER_t	Energy Efficiency Ratio of the air-to-air HP [−]
FCF	Flow Correction Factor [−]
HC_{mCHP}	Heating capacity from mCHP [kW_{th}] or Heating demand from building covered by mCHP [kW_{th}]
f_{el}	Emission factor of electricity [kg_{CO2}/kWh_e]
f_{ng}	CO_2 emission factor of natural gas [kg_{CO2}/kWh_{th}]
HIF	Heating Input Factor [−]
I_0	Diode reverse saturation current
I_{DC}	Annual cooling covered demand index [%]
I_{DH}	Annual thermal covered demand index [%]
I_{ESS}	Annual energy self-sufficiency index [%]
i_f	Fuel inflation rate [%]
I_L	Light current [A]
LCS	Life Cycle Cost Saving [k€]
LCOE	Levelized Cost Of Energy [€/kWh_e]
I_{PSC}	Annual physical self-consumption index [%]
I_{TSC}	Total self-consumption index [%]
I_{TSS}	Annual thermal self-sufficiency index [%]
I_{VSC}	Annual virtual self-consumption index [%]
PBT	Payback Time [y]
Pc	Electrical power withdrawn for the elevator, the lighting and the equipment from the condominium (common use) [kW_e]
$Pc_€$	Physical self-consumption power consumed [kW_e]
P_{EVAP}	Cooling capacity of the evaporator [$kW_{f]}$]
P_{GEN}	Heat input of generator [$kW_{th]}$]
$Pn_€$	Net electrical power produced and fed into the grid by the RES plants
P_P	Total power produced by RES [kW_e]
$Ps_€$	Shared power [kW_e]
$P_{u\ tot}$	Electrical power withdrawn from the zones [kW_e]
Pz	Zonal price [€/kWh_e]
RCC	Rated cooling capacity of the evaporator [kW_f]
RHI	Rated heat input of the generator [kW_{th}]
R_s	Series resistance [Ω]
R_{sh}	Shunt resistance [Ω]
SoC	State Of Charge [%]
t	Sub-hourly period (simulation *timestep*) [h]
T_{CND}	Temperature of condenser (air-to-air HP) [°C]
T_{EVAP}	Temperature of evaporator (air-to-air HP) [°C]
T_{ARERA}	ARERA incentive tariff [€/kWh_e]
T_P	Incentive tariff [€/kWh_e]
$TRAS_E$	Tariff for the transmission service [€/kWh_e]
WWR	Window-Wall-Ratio [%]
X_P	Hours of operation [h]
Y_P	Size that maximizes the hours of operation along the cumulative energy curve [kW_e] or [kW_{th}] if referred to mCHP or [kW_f] if referred to WFAC
Greek Letters	
α	Ideality factor [−]
Δ	Difference between microgrid and building demands (heating, cooling and electric)
η_{boil}	boiler efficiency [−]

Subscripts/superscript

0	Referred to capital cost/diode reverse saturation current
€	Referred to the revenue produced by energy sharing, self-consuming and RID
absorption chiller	Referred to cooling demand covered by WFAC
avoid el HP	Referred to electric energy saved (heating)
avoid ng	Referred to thermal energy saved (heating)
building	Referred to heating, cooling and electric demand of the building
c	Referred to electrical power withdrawn for common use in the condominium
CND	Referred to condenser of air-to-air HP
cov	Referred to covered demand by mCHP (heating)/WFAC (cooling)
DC	Referred to cooling demand
DH	Referred to heating demand
e	Referred to electric energy
el	Referred to electrical
ESS	Referred to annual energy self-sufficiency index
EVP	Referred to evaporator of the WFAC/air-to-air HP
f	Referred to cooling energy/Fuel inflation rate
GEN	Referred to generator of the *WFAC*
L	Referred to light current

(*continued on next page*)

(*continued*)

mCHP	Referred to Micro Combined Heat and Power
microgrid	Referred to electric demand from microgrid
net	Referred to annual benefits
ng	Referred to natural gas
O&M	Referred to Operation and maintenance
p	Referred to the total power produced by RES or the size or the hours of operation along the cumulative energy curve
PSC	Referred to the annual physical self-consumption index
s	Referred to series resistance
sh	Referred to shunt resistance
tot	Referred to total
TSC	Referred to the total self-consumption index
TSS	Referred to the annual thermal self-sufficiency index
th	Referred to the heating energy
ui	Referred to single zone
u tot	Referred to zones
VSC	Referred to the annual virtual self-consumption index
WFAC	Referred to water-fired absorption chiller

Data availability

Data will be made available on request.

References

[1] Alam MR, St-Hilaire M, Kunz T. Peer-to-peer energy trading among smart homes. Appl Energy 2019;238:1434–43. https://doi.org/10.1016/J.APENERGY.2019.01.091.

[2] Office of the European Union P. Clean energy for all Europeans energy. https://doi.org/10.2833/21366; 2019.

[3] Biresselioglu ME, Limoncuoglu SA, Demir MH, Reichl J, Burgstaller K, Sciullo A, et al. Legal provisions and market conditions for energy communities in Austria, Germany, Greece, Italy, Spain, and Turkey: a comparative assessment. Sustainability 2021;13:11212. https://doi.org/10.3390/su132011212.

[4] European Commission. Directive (EU) 2018/2001 of the European Parliament and of the Council of 11 December 2018 on the promotion of the use of energy from renewable sources. Available at: https://eur-lex.europa.eu/eli/dir/2018/2001/oj; [Accessed 13 May 2025].

[5] Eriksson Berggren S, Witt T, Van der Linden E, Saes L, Arvefjord LE, Heckenberg D, et al. Energy communities. Nordic Energy Res 2023. https://doi.org/10.6027/NER2023-03.

[6] Williams Annabel Clean energy from the ground up: energy communities in the European Union. Clean Air Task Force (CATF) 2024. Available at: https://www.catf.us/resource/clean-energy-ground-up-energy-communities-european-union/. [Accessed 13 May 2025].

[7] Rosales-Asensio E, Diez DB, Cabrera P, Sarmento P. Effectiveness and efficiency of support schemes in promoting renewable energy sources in the Spanish electricity market. Int J Electr Power Energy Syst 2024;158:109926. https://doi.org/10.1016/j.ijepes.2024.109926.

[8] Minister of Economy and Finance. Decreto Legge 30 dicembre 2019, n. 162 Disposizioni urgenti in materia di proroga di termini legislativi, di organizzazione delle pubbliche amministrazioni. nonchè di innovazione tecnologica 2019;162. Available at: https://www.normattiva.it/uri-res/N2Ls?urn:nir:stato:decreto.legge:2019-12-30. [Accessed 13 May 2025].

[9] Decree of the Minister of Economic Development (MISE). Individuazione della tariffa incentivante per la remunerazione degli impianti a fonti rinnovabili inseriti nelle configurazioni sperimentali di autoconsumo collettivo e comunita' energetiche rinnovabili. attuazione dell'articolo 42-bis; 2020. Decreto 16 settembre 2020, comma 9, del decreto-legge n. 162/2019, convertito dalla legge n. 8/2020. Available at: https://www.gazzettaufficiale.it/eli/id/2020/11/16/20A06224/sg. [Accessed 13 May 2025].

[10] Decree of the Minister of Environment and Energy Security (MASE). Decreto Legge n. 414 del 7 dicembre 2023, recante: individuazione di una tariffa incentivante per impianti a fonti rinnovabili inseriti in comunita' energetiche rinnovabili e nelle configurazioni di autoconsumo singolo a distanza e collettivo. attuazione del decreto legislativo 8 novembre 2021, n.199 e in attuazione della misura appartenente alla Missione 2, Componente del 2, Investimento 1.2 del PNRR. 2023. Available at: https://www.gazzettaufficiale.it/eli/id/2024/02/07/24A00671/sg#:~:text=414%20del%207%20dicembre%202023,legislativo%208%20novembre%202021%2C%20n. [Accessed 13 May 2025].

[11] Autorità di Regolazione per Energia Reti e Ambiente (ARERA). Delibera 30 gennaio 2024 15/2024/R/eel, Modifiche al Testo Integrato Autoconsumo Diffuso e verifica delle Regole Tecniche per il servizio per l'autoconsumo diffuso predisposte dal Gestore dei Servizi Energetici S. Available at: https://www.arera.it/atti-e-provvedimenti/dettaglio/24/15-24; [Accessed 13 May 2025].

[12] Plaza C, Gil J, de Chezelles F, Strang KA. Distributed solar self-consumption and blockchain solar energy exchanges on the public grid within an energy community. 2018 IEEE international conference on environment and electrical engineering and 2018 IEEE industrial and commercial power systems Europe (EEEIC/I&CPS Europe). IEEE; 2018. p. 1–4. https://doi.org/10.1109/EEEIC.2018.8494534.

[13] Fleischhacker A, Lettner G, Schwabeneder D, Auer H. Portfolio optimization of energy communities to meet reductions in costs and emissions. Energy 2019;173:1092–105. https://doi.org/10.1016/j.energy.2019.02.104.

[14] Fina B, Fleischhacker A, Auer H, Lettner G. Economic assessment and business models of rooftop photovoltaic systems in multiapartment buildings: case studies for Austria and Germany. J Renew Energy 2018;2018:1–16. https://doi.org/10.1155/2018/9759680.

[15] Ceglia F, Marrasso E, Samanta S, Sasso M. Addressing energy poverty in the energy community: assessment of energy, environmental, economic, and social benefits for an Italian residential case study. Sustainability 2022;14:15077. https://doi.org/10.3390/su142215077.

[16] Dal Cin E, Carraro G, Volpato G, Lazzaretto A, Danieli P. A multi-criteria approach to optimize the design-operation of energy communities considering economic-environmental objectives and demand side management. Energy Convers Manag 2022;263:115677. https://doi.org/10.1016/j.enconman.2022.115677.

[17] Giordano A, Mastroianni C, Scarcello L, Spezzano G. An optimization model for efficient energy exchange in energy communities. 2020 fifth international conference on fog and Mobile edge computing (FMEC). IEEE; 2020. p. 319–24. https://doi.org/10.1109/FMEC49853.2020.9144901.

[18] Ceglia F, Marrasso E, Martone C, Pallotta G, Roselli C, Sasso M. Towards the decarbonization of industrial districts through renewable energy communities: techno-economic feasibility of an Italian case study. Energies 2023;16:2722. https://doi.org/10.3390/en16062722.

[19] Battaglia V, Vanoli L, Zagni M. Economic benefits of renewable energy communities in smart districts: a comparative analysis of incentive schemes for NZEBs. Energy Build 2024;305:113911. https://doi.org/10.1016/j.enbuild.2024.113911.

[20] Cirone D, Bruno R, Bevilacqua P, Perrella S, Arcuri N. Techno-economic analysis of an energy community based on PV and electric storage systems in a small Mountain locality of south Italy: a case study. Sustainability 2022;14:13877. https://doi.org/10.3390/su142113877.

[21] Fouladvand J, Ghorbani A, Mouter N, Herder P. Analysing community-based initiatives for heating and cooling: a systematic and critical review. Energy Res Social Sci 2022;88:102507. https://doi.org/10.1016/j.erss.2022.102507.

[22] Papatsounis AG, Botsaris PN, Katsavounis S. Thermal/cooling energy on local energy communities: a critical review. Energies 2022;15:1117. https://doi.org/10.3390/en15031117.

[23] Ceglia F, Marrasso E, Roselli C, Sasso M, Coletta G, Pellegrino L. Biomass-based renewable energy community: economic analysis of a real case study. Energies 2022;15:5655. https://doi.org/10.3390/en15155655.

[24] Kim M-H, Kim D, Heo J, Lee D-W. Techno-economic analysis of hybrid renewable energy system with solar district heating for net zero energy community. Energy 2019;187:115916. https://doi.org/10.1016/j.energy.2019.115916.

[25] Ancona MA, Baldi F, Branchini L, De Pascale A, Gianaroli F, Melino F, et al. Comparative analysis of renewable energy community designs for district heating networks: case study of Corticella (Italy). Energies 2022;15:5248. https://doi.org/10.3390/en15145248.

[26] Ceglia F, Marrasso E, Roselli C, Sasso M. Small renewable energy community: the role of energy and environmental indicators for power grid. Sustainability 2021;13:2137. https://doi.org/10.3390/su13042137.

[27] Ceglia F, Marrasso E, Roselli C, Sasso M. Energy and environmental assessment of a biomass-based renewable energy community including photovoltaic and hydroelectric systems. Energy 2023;282:128348. https://doi.org/10.1016/j.energy.2023.128348.

[28] Kalinci Y, Hepbasli A, Dincer I. Techno-economic analysis of a stand-alone hybrid renewable energy system with hydrogen production and storage options. Int J Hydrogen Energy 2015;40:7652–64. https://doi.org/10.1016/j.ijhydene.2014.10.147.

[29] Kotowicz J, Uchman W. Analysis of the integrated energy system in residential scale: Photovoltaics, micro-cogeneration and electrical energy storage. Energy 2021;227:120469. https://doi.org/10.1016/j.energy.2021.120469.
[30] Tabriz ZH, Khani L, Mohammadpourfard M, Akkurt GG. Biomass driven polygeneration systems: a review of recent progress and future prospects. Process Saf Environ Prot 2023;169:363–97. https://doi.org/10.1016/j.psep.2022.11.029.
[31] Di Fraia S, Shah M, Vanoli L. Biomass polygeneration systems integrated with buildings: a review. Sustainability 2024;16:1654. https://doi.org/10.3390/su16041654.
[32] Klein MJDSA, Beckman WA, Mitchell JW, Duffie JA, Duffie NA, Freeman TL, et al. Trnsys17. 2009.
[33] Doumen SC, Nguyen P, Kok K. Challenges for large-scale local electricity market implementation reviewed from the stakeholder perspective. Renew Sustain Energy Rev 2022;165:112569. https://doi.org/10.1016/j.rser.2022.112569.
[34] Cutore E, Volpe R, Sgroi R, Fichera A. Energy management and sustainability assessment of renewable energy communities: the Italian context. Energy Convers Manag 2023;278:116713. https://doi.org/10.1016/j.enconman.2023.116713.
[35] Trimble Inc. SketchUp. Available at: https://www.sketchup.com/en;[Accessed 13 May 2025].
[36] U.S. department of energy commercial reference building models of the national building stock. 2011. Available at: http://www.osti.gov/bridge. [Accessed 13 May 2025].
[37] Ente Nazionale Italiano di Unificazione (UNI). UNI/TR 11552:2014, opaque envelope components of buildings - thermo-physical parameters. 2014. Available at: https://store.uni.com/en/uni-tr-11552-2014. [Accessed 13 May 2025].
[38] Cardona E, Piacentino A, Cardona F. Energy saving in airports by trigeneration. Part I: assessing economic and technical potential. Appl Therm Eng 2006;26:1427–36. https://doi.org/10.1016/j.applthermaleng.2006.01.019.
[39] Cardona E, Piacentino A. A methodology for sizing a trigeneration plant in mediterranean areas. Appl Therm Eng 2003;23:1665–80. https://doi.org/10.1016/S1359-4311(03)00130-3.
[40] La Villetta M, Costa M, Cirillo D, Massarotti N, Vanoli L. Performance analysis of a biomass powered micro-cogeneration system based on gasification and syngas conversion in a reciprocating engine. Energy Convers Manag 2018;175. https://doi.org/10.1016/j.enconman.2018.08.017.
[41] Barisano D. Biomass and Waste Gasification Country Report ITALY. IEA Bioenergy Task 33; 2018. Available at: https://task33.ieabioenergy.com/wp-content/uploads/sites/33/2022/06/ITALY2018.pdf. [Accessed 13 May 2025].
[42] Costruzioni Motori Diesel S.p.A. (CMD). ECO20x CHP System 2024. Available at: https://wwwEco20cmdCom/En/Eco20x/ [Accessed 13 May 2025].
[43] Caputo C, Cirillo D, Costa M, Villetta ML, Tuccillo R, Villani R. Numerical analysis of a combined heat and power generation technology from residual biomasses. Journal of Energy and Power Engineering 2018;12:300–21. https://doi.org/10.17265/1934-8975/2018.06.003.
[44] Piazzullo D, Costa M, Calise F, Vicidomini M, Dentice d'Accadia M. Technical, economic and environmental feasibility of a real hybrid mCHP system based on residual biomass gasification and solar PV: a transient numerical study. Proceedings of Venice 2020, 8th international symposium on energy from biomass and waste. Venice: Cisa Publisher; 2020.
[45] Costa M, Piazzullo D, Cappiello FL, Calise F, Vicidomini M, Dendice d'Accadia M. A transient model of a hybrid system based on biomass gasification and PV for combined cooling, heat and power for electric mobility services. 16th sustainable development of energy, water and environment systems. Croatia: Dubrovnik; 2021.
[46] Barisano D, Bianco L, Nanna F, Pierro N, Villone A, Cirillo D, et al. Efficient micro-grids powered by only renewable source for the energy autonomy of rural areas - EMERA project. 31st Eur Biomass Conf Exhibit 2023;4:716–25. https://doi.org/10.5071/31stEUBCE2023-4BV.5.19. Bologna (Italy).
[47] Costa M, Piazzullo D, Di Battista D, De Vita A. Sustainability assessment of the whole biomass-to-energy chain of a combined heat and power plant based on biomass gasification: biomass supply chain management and life cycle assessment. J Environ Manag 2022;317:115434. https://doi.org/10.1016/j.jenvman.2022.115434.
[48] MAYA. Water fired absorption chillers WFC series, Model: WFC SC 5 2024. Available at:https://wwwMaya-AirconditioningCom/Wp-Content/Uploads/2022/10/WFC-Series-LD_001_ENPdf [Accessed 13 May 2025].
[49] De Soto W, Klein SA, Beckman WA. Improvement and validation of a model for photovoltaic array performance. Sol Energy 2006;80:78–88. https://doi.org/10.1016/j.solener.2005.06.010.
[50] Sadio OD, Kouyaté M, Traoré PT, Barro FI. Determination of the electrical parameters of a solar cell in steady state. Open J Appl Sci 2023;13:1834–43. https://doi.org/10.4236/ojapps.2023.1310144.
[51] Eging P.V. EG-(SERIES) M54-HLV 405Wp technical datasheet. Available at: https://wwwGingroupIt/Prodotto/Eging-Pv-Eg-Seriesm54-Hlv-405wp [Accessed 13 May 2025].
[52] EASE. Electrochemical Energy Storage. Lithium-Ion Battery Technical Datasheet. 2024. Available at: https://www Ease-StorageEu/Wp Content/Uploads/2016/03/EASE_TD_LiIonPdf. [Accessed 13 May 2025].
[53] Wang K, Herrando M, Pantaleo AM, Markides CN. Technoeconomic assessments of hybrid photovoltaic-thermal vs. conventional solar-energy systems: case studies in heat and power provision to sports centres. Appl Energy 2019;254:113657. https://doi.org/10.1016/j.apenergy.2019.113657.
[54] CLIVET. Performance data based on UNITS 11300 – 3, 4 2024. Available at: https://www.schede-tecniche.it/schede-tecniche-climatizzatori/CLIVET-scheda-prodotto-condizionatore-CRISTALLO.pdf [Accessed 13 May 2025].
[55] Thomas Huld IP-P Global irradiation and solar electricity potential in Italy. European Commission: Joint Research Centre Institute for Energy and Transport, Renewable Energy Unit. 2025. Available at: https://re.jrc.ec.europa.eu/pvg_download/map_pdfs/G_hor_IT.pdf. [Accessed 13 May 2025].
[56] Shabbir N, Kutt L, Astapov V, Jawad M, Allik A, Husev O. Battery size optimization with customer PV installations and domestic load profile. IEEE Access 2022;10:13012–25. https://doi.org/10.1109/ACCESS.2022.3147977.
[57] Chatzigeorgiou NG, Theocharides S, Makrides G, Georghiou GE. A review on battery energy storage systems: applications, developments, and research trends of hybrid installations in the end-user sector. J Energy Storage 2024;86:111192. https://doi.org/10.1016/j.est.2024.111192.
[58] Correa-Jullian C, Crespo A, Cortés F, Ibarra M. Simulation of a solar fired absorption system for a case study in the dairy industry. Proceedings of EuroSun 2018. Freiburg, Germany: International Solar Energy Society; 2018. p. 1–10. https://doi.org/10.18086/eurosun2018.04.16.
[59] Soteris A. Kalogirou. Solar energy engineering. Elsevier; 2014. https://doi.org/10.1016/C2011-0-07038-2.
[60] Eurostat. Electricity prices for household consumers. Available at: https://EcEuropaEu/Eurostat/Databrowser/View/Nrg_pc_204/Default/Table?Lang=en [Accessed 13 May 2025].
[61] Eurostat. Gas prices for household consumers. Available at: https://EcEuropaEu/Eurostat/Databrowser/View/Nrg_pc_202/Default/Table?Lang=en [Accessed 13 May 2025].
[62] Italian Institute for Environmental Protection and Research (ISPRA). Emission factors for the production and consumption of electricity in Italy. 2025. Available at: https://emissioni.sina.isprambiente.it/inventario-nazionale/#Report. [Accessed 13 May 2025].
[63] Italian Institute for Environmental Protection and Research (ISPRA). Fattori di emissione atmosferica di CO2 e altri gas a effetto serra nel settore elettrico. 2025. Available at: https://www.isprambiente.gov.it/files2017/pubblicazioni/rapporto/R_257_17.pdf. [Accessed 13 May 2025].
[64] Bertolini M, Duttilo P, Lisi F. Accounting carbon emissions from electricity generation: a review and comparison of emission factor-based methods. Appl Energy 2025;392:125992. https://doi.org/10.1016/j.apenergy.2025.125992.
[65] Hassan Q. Evaluate the adequacy of self-consumption for sizing photovoltaic system. Energy Rep 2022;8:239–54. https://doi.org/10.1016/j.egyr.2021.11.205.
[66] Menin L, Paolillo A, Piazzi S, Antolini D, Ravazzolo F, Baratieri M. Biomass derived combined heat and power from decentralized small-scale gasification: updated cost conditions for the Italian Mountain context and competitiveness in future energy markets. Waste Biomass Valoriz 2025;16:4009–25. https://doi.org/10.1007/s12649-025-02948-3.
[67] Rudello G. Prezzo del cippato a settembre 2025. https://energiadallegno.it/prezzo-del-cippato-a-settembre-2025/. [Accessed 13 May 2025].
[68] Italian Agroforestry Energy Association (AIEL). Gruppo produttori professionali biomnasse. 2025. Available at: https://www.aielenergia.it/gruppo-home-GPPB. [Accessed 13 May 2025].